PERGAMON

Journal of South American Earth Sciences, Vol. 11, No. 6, pp. 533–560, 1998

Printed in Great Britain
PII: S0895-9811(98)00031-5
0895-9811/98/$ - see front matter

Climatic and tectonic implications of the late Miocene Jakokkota flora, Bolivian Altiplano

[1]KATHRYN M. GREGORY-WODZICKI*, [2]W.C. MCINTOSH and [3]KATTIA VELASQUEZ

[1]Lamont-Doherty Earth Observatory of Columbia University, Palisades, NY 10964-8000, USA
[2]New Mexico Bureau of Mines and Mineral Resources, Socorro, NM, USA
[3]Carrera de Geología, Universidad Mayor de San Andres, La Paz, Bolivia

Abstract — When compared to a database of modern foliar physiognomy and climate, the physiognomy of a new collection of dicotyledonous leaves from the 10.66 ± 0.06 Ma Jakokkota flora, Bolivian Altiplano, implies a mean annual temperature (MAT) of $18.6–21.0 \pm 2.5°C$. Similarly, a literature-derived sample of the early-middle Miocene Potosí flora, Cordillera Oriental, implies a MAT of $21.5–21.7 \pm 2.1°C$. We estimate that both floras experienced a growing season precipitation of 50 ± 40 cm. The paleoclimate thus appears considerably warmer than the current highland climate, with MATs of 8–9°C; the paleoprecipitation is indistinguishable from modern levels. A comparison of the Miocene MATs with the modern MATs, with the effects of latitudinal continental drift and global climate change subtracted, suggests that the Jakokkota flora grew at an elevation of $590–1610 \pm 1000$ m, and the Potosí flora grew at an elevation of $0–1320 \pm 1000$ m. Both paleoelevation estimates are significantly lower than the present elevations of 3940 and 4300 m, respectively, requiring a substantial component of Andean uplift since 10.7 Ma. This uplift history is consistent with two-stage tectonic models of Andean orogeny. © 1998 Elsevier Science Ltd. All rights reserved

Resumen — La fisiognomía de una nueva colección de hojas dicotiledoneas de la flora Jakokkota, Altiplano de Bolivia, de 10.66 ± 0.06 Ma de edad, implica un promedio anual de temperatura (PAT) de $18.6–21.0 \pm 2.5°C$, si la compara a un base de datos de fisiognomía moderna y el clima. Similarmente, una muestra derivada de la literatura de la flora Potosí, Cordillera Oriental, de edad Mioceno temprano o medio, implica un PAT de $21.5–21.7 \pm 2.1°C$. Estimamos que las dos floras experimentaron una precipitación durante la estación de crecimiento de las plantas de 50 ± 40 cm. Entonces, parece que el paleoclima era mas caliente que el clima actual de terreno montañoso, con PATs de 8–9°C; la paleoprecipitación no era muy diferente de los niveles actuales. Una comparación de los PATs Miocenos con los PATs modernos, con los efectos de la deriva de los continentes y el cambio global de clima sustraidos, sugiere que la flora Jakokkota creció a una altura de $590–1610 \pm 1000$ m, y la flora Potosí creció a una altura de $0–1320 \pm 1000$ m. Las dos estimaciones son significativamente mas bajas que las alturas actuales de 3940 y 4300 m, respectativamente, requiriendo un componente substancial de solevantamiento desde 10.7 Ma. Esta historia de solevantamiento está de acuerdo con los modelos tectonicos de la orogenia Andina de dos etapas. © 1998 Elsevier Science Ltd. All rights reserved

INTRODUCTION

In the early part of the 20th century, E. W. Berry studied a number of Neogene fossil floras from the Altiplano and Cordillera Oriental of Bolivia (Berry, 1919, 1922a,b, 1939; Singewald and Berry, 1922). The Altiplano, with an average elevation of 3700 m (Isacks, 1988), is the second highest and largest plateau in the world after the Tibetan plateau. The ranges and intermontane valleys of the Cordillera Oriental bound the Altiplano to the east (Fig. 1).

The Altiplano is located in the tropics, but due to the high elevations, the climate is temperate and dry, and vegetation is sparse (Johnson, 1976). The paleofloras Berry studied were much more diverse than the modern tundra-like vegetation, and he interpreted that they grew under a warmer, wetter climate. Taking into account evidence of faulting and folding in young rocks, he further surmised that the paleoclimate of the floras was closely tied to the paleoelevation, and thus the warm temperatures suggested lower elevations than at present (Berry, 1919, 1922a,b).

However, the reliability of these interpretations is questionable. They are based on the identification to species of sparse fossil material; also, Berry tended to identify to North American genera, even though the Central American land bridge did not develop until considerably after the floras had lived. In order to estimate paleoclimate and elevation, he equated the environmental ranges of the closest living relatives to the fossil species with the environmental ranges of the fossil species, an assumption that has been criticized (Wolfe, 1971; Wolfe and Schorn, 1990; Chaloner and Creber, 1990).

More than 50 years after Berry's work, we know nothing further about the Oligocene, Miocene, and Pliocene paleotemperatures of the high central Andes, and most subsequent attempts to estimate Neogene paleoelevations (Tosdal *et al.,* 1984; Benjamin *et al.,* 1987; Alpers and Brimhall, 1988; Gubbels *et al.,* 1993; Vandervoort *et al.,* 1995; Kennan *et al.,* 1997; Lamb and Hoke, 1997) involve large assumptions, lack error

* Corresponding author.

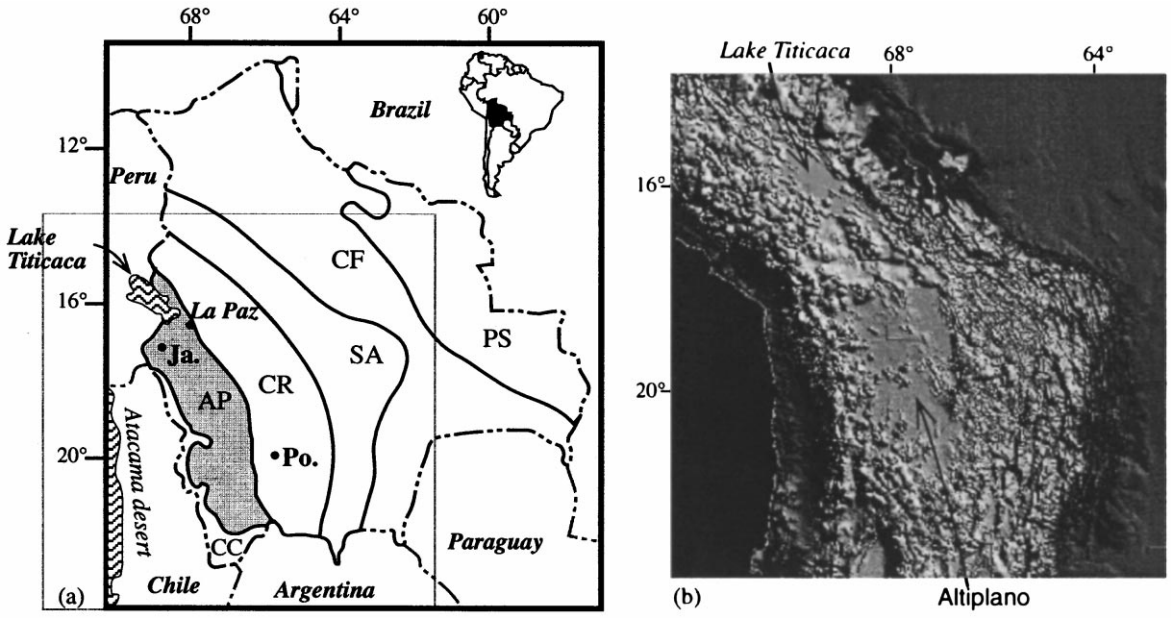

Fig. 1. Location map of study area, with physiographic provinces (capital letters): CC = Cordillera Occidental; AP = Altiplano (shaded); CR = Cordillera Oriental; SA = Subandean Fold-Thrust Belt; CF = Chaco Foreland (and Beni Plain); PS = Precambrian Shield; and fossil floras (dots): Ja. = Jakokkota; Po. = Potosí. Wavy lines indicate water. Light gray box shows the location of (b), USGS 30 arc-second DEM data for the Central Andes, as processed by the Cornell Andes Project.

analyses, or use methods subject to contention (England and Molnar, 1990; Gregory and Chase, 1994; Chase *et al.,* 1998; Gregory, in preparation).

In the past decade, new and, we argue, improved ways of determining the paleoclimate and paleoelevation of fossil floras have been developed. The foliar physiognomic method of Wolfe (1995) uses modern relationships between climate and leaf morphology/anatomy to derive quantitative estimates of past climate, and modern relationships between climate variables and elevation are used to estimate paleoelevation (Wolfe, 1992; Forrest *et al.,* 1995, in press). Thus it is worth revisiting the floras of Berry.

In this study, we use the foliar physiognomic method to analyze a new collection of dicotyledonous leaves from the late Miocene Jakokkota flora from the northern Altiplano, and a sample from the literature of the early to middle Miocene Potosí flora (Berry, 1939), located in the Cordillera Oriental. A detailed description of the Jakokkota sample is given in the Appendix.

The resulting paleoclimate and paleoelevation estimates can be used to understand the Miocene climatic and tectonic evolution of the high central Andes. Because of the large errors for the paleoelevation estimates (~700–1000 m), they are ideally analyzed as part of a large dataset, rather than as individual datapoints (i.e. Wolfe *et al.,* 1997; Chase *et al.,* 1998). However, such an analysis is not possible, given the dearth of studies of South American floras, and of other reliable paleoelevation estimates.

The botanically derived paleoelevations are still useful, because they constrain first-order elevation, that is, whether the floras grew at sea-level, an intermediate elevation, or modern elevations of ~400 m. Such information is necessary to constrain boundary conditions for general circulation models (GCMs); comparisons of GCM simulations with and without the Cordillera suggest that the Andes have a dramatic effect on precipitation and temperature over and near South America (Walsh, 1994; Lenters and Cook, 1995; Lenters *et al.,* 1995).

In this study, the paleoelevation estimates are used to evaluate proposed models of Andean evolution (Molnar and Lyon-Caen, 1988; Allmendinger *et al.,* 1997; Lamb *et al.,* 1997; Okaya *et al.,* 1997). Understanding Andean deformation is especially important, because the Andes are the type example of an ocean-continent subduction zone with associated crustal deformation. A deeper understanding of the modern Andes will further our understanding of ancient analogous orogens, such as the Cretaceous–early Cenozoic North American Cordillera (Jordan *et al.,* 1983; Coney and Evenchick, 1994).

GEOLOGY AND STRATIGRAPHY OF THE JAKOKKOTA SITE

The Altiplano is generally defined as the large area of moderate relief and internal drainage in the highlands of the central Andes; elevations are between 3500 and 4700 m (Isacks, 1988) (Fig. 1). It is bounded on the west by the Cordillera Occidental, an active volcanic arc, and to the east by the Cordillera Oriental, an inactive fold and thrust belt. Further to

the east is found the active fold and thrust-belt of the Subandean zone and the Chaco foreland basin.

The Jakokkota flora is located in the northern Altiplano about 100 km SW of the capital, La Paz, and just east of the border with Peru near the town of Santiago de Machaca (Fig. 2). It crops out on Cerro Jakokkota, at an elevation of approximately 3940 m.

The flora was deposited in member 6 of the Miocene Mauri Formation, a 410 m thick sequence of fluvial and lacustrine sediments with intercalated tuffs (Sirvas and Torres, 1966; GEOBOL, 1994; Suarez and Diaz, 1996). Fossil leaves and seeds are found in a white, ash-rich claystone to fine-grained sandstone layer, which is overlain by a gray, coarse-grained, volcaniclastic sandstone (Fig. 3). The fossiliferous layer is only present in one canyon (Fig. 4), probably due to erosion during the deposition of the overlying layer. This locality is the same as that pictured in Berry (1922a).

The contact between the fossiliferous layer and the overlying coarse sandstone is very irregular, often displaying flame structures (Fig. 4), which are indicative of soft-sediment loading. The fossiliferous layer is generally graded, with an up to 60 cm fine-grained sandstone below, and an up to 25 cm siltstone–claystone with hackly fracture above (Fig. 3). Fossil material is only found in the upper siltstone–claystone layer.

The upper siltstone–claystone has finely alternating organic-rich and organic-poor layers, which indicates that it is not a primary volcanic ash, but was reworked, probably by a low energy stream. Generally the organic-rich layers consist of very fine-grained leaf, bark, and seed fragments. However, the uppermost layers contain much larger fragments and often complete leaves. Occasionally fossil leaves are found half in tuffaceous silt-claystone, and half in the overlying unit, suggesting, like the flame structures, that the deposition of the two units was close in time.

This coarser organic-rich layer was the primary source of the fossil leaves collected in this study. Because of the erosion/loading associated with the

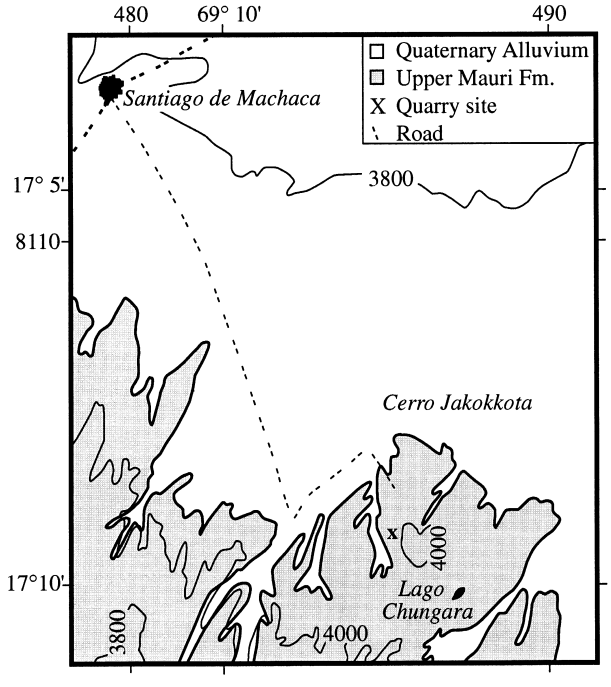

Fig. 2. Geological map of Cerro Jakokkota area. Redrawn from GEOBOL (1994).

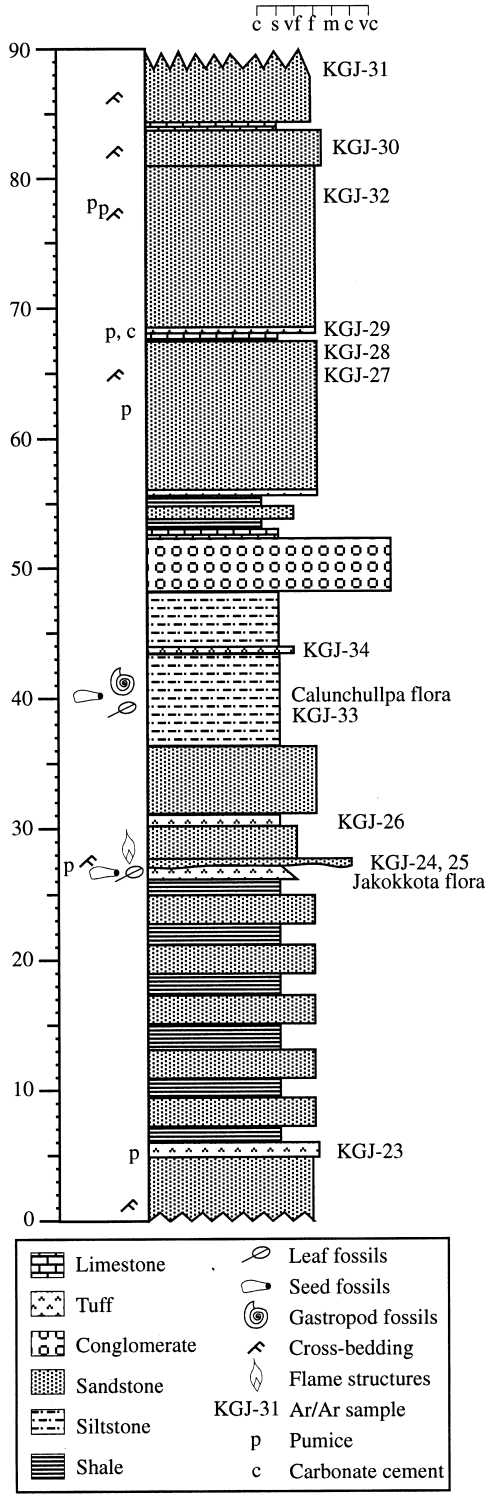

Fig. 3. Generalized stratigraphic column for Cerro Jakokkota.

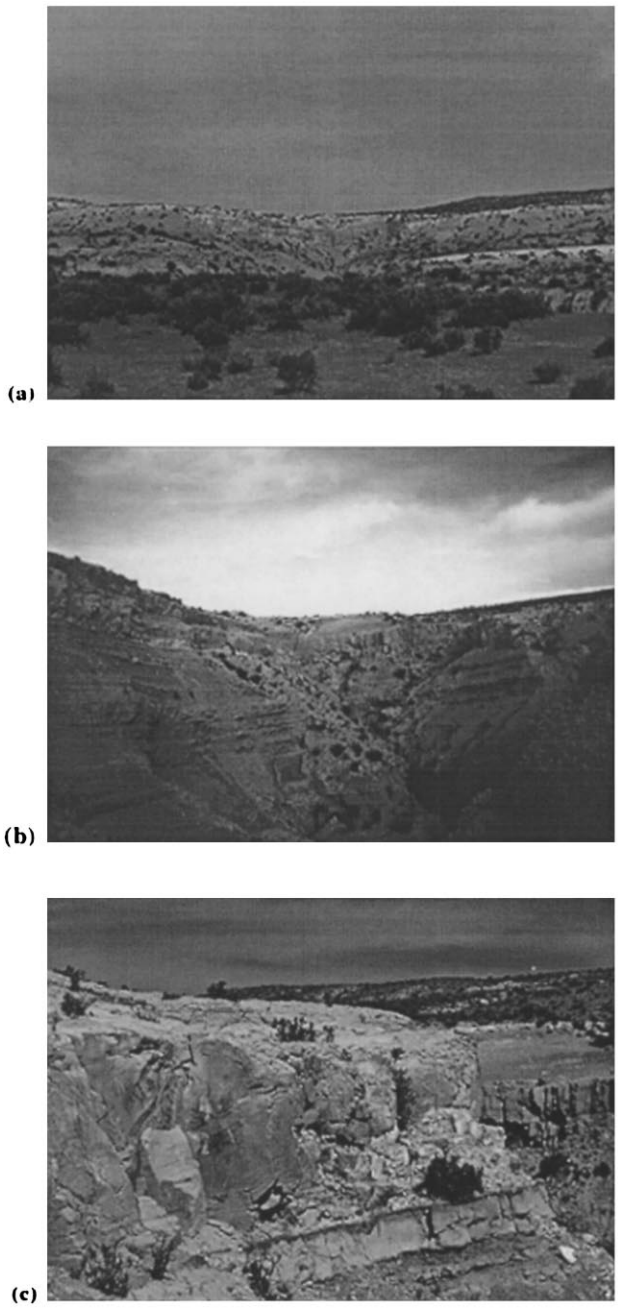

Fig. 4. Photos of Cerro Jakokkota and the fossil locality. (a) Cerro Jakokkota, looking east, showing the quebrada where the fossiliferous layer crops out. (b) Close-up of the quebrada (compare with photo of Berry (1922a, p. 206). The fossiliferous layer is the lower (white) part of the cliff-forming layer just below the top. (c) Close up of fossiliferous layer (white layer with prominent flame structures) and overlying sandstone. The fall ash from which the sample KGJ-26 was collected is the thin, white layer on the opposite side of the quebrada.

overlying sandstone unit, this layer is only present over about 5 m of exposure.

Another flora, named here the Calunchullpa flora, and gastropod fossils are found in lacustrine beds above the Jakokkota locality (Fig. 3). This flora will be described in a subsequent paper.

Marshall *et al.* (1992) obtained a $^{40}Ar/^{39}Ar$ date of 11.42 ± 0.21 Ma from biotite on a tuff in member 6 from Cerro Jakokkota that they describe as stratigraphically above the fossiliferous unit of Berry (1922a). They correlate this tuff with the Ulloma Tuff, which has a better constrained sanidine-based date of 10.35 ± 0.06 Ma. However, Marshall *et al.* (1992) do not show the stratigraphic location of their sample, so we dated tuffaceous layers near the plant beds in order to put the fossiliferous layers and the tuffs in the same stratigraphic context.

$^{40}Ar/^{39}Ar$ methods

Hand samples for $^{40}Ar/^{39}Ar$ analysis, consisting typically 1–5 kg of unweathered, unaltered rock, were collected from 11 layers of volcaniclastic sandstone, ash fall, and lapilli fall of member 6 of the Mauri Formation (Fig. 3). The sandstone layers were cross-bedded, indicating that they are fluvial in origin. Six of the sampled layers contained datable minerals; K-feldspar bearing separates were obtained from 4 samples, and biotite/hornblende were obtained from 2 samples.

Hand samples were also collected from volcaniclastic sandstone layers interbedded with the fossil-leaf bearing shales of the Caracoles tuff at Potosí, along with a sanidine-ignimbrite which is in fault contact with the overlying fossil-bearing shales. K-feldspar bearing separates were obtained from the ignimbrite, but none of the sandstones contained datable material.

K-feldspar separates were prepared by hand-picking pumice clasts, washing them, crushing and sieving to 125 μm–1 mm, ultrasonic cleaning these grains in dilute (7%) hydrofluoric acid, then applying magnetic and density-liquid techniques followed by hand picking. Aliquots of feldspar separates (10–20 mg) were packaged with alternating flux monitors of Fish Canyon Tuff sanidine (27.84 Ma relative to Mmhb-1 hornblende at 520.4 Ma; Samson and Alexander, 1987) and irradiated in the D3 position of the reactor at Texas A & M University.

$^{40}Ar/^{39}Ar$ analyses were performed at the New Mexico Geochronology Research Laboratory at the New Mexico Institute of Mining and Technology. This facility includes an MAP 215-50 mass spectrometer attached to a fully automated all-metal argon extraction system equipped with a 10 W CO_2 laser. Monitor sanidine crystals and sanidine crystals from the Potosí samples were large enough to allow laser-fusion analysis of single grains. Typically 8–12 grains from each sample were individually analyzed. Because of their small size, crystals in most of the Jakokkota samples were run by laser fusion of 3–10 grains. In the case of sample KGJ-26, 10–30 crystal aliquots were fused for each of the six analyses. Samples and monitors were fused by CO_2 laser for 15 s, then reactive gasses were removed using a SAES GP-50 getter prior to expansion into the mass spec-

trometer. Extraction line blanks during these analyses averaged 200, 2, 0.6, 2, and 3×10^{-18} moles at masses 40, 39, 38, 37, and 36, respectively. The neutron flux values (J values) within irradiation packages were determined to a precision of $\pm 0.1\%$ by CO_2 laser-fusion of 4 single crystals from each of 4 or 6 radial positions around each irradiation tray.

$^{40}Ar/^{39}Ar$ results

The results are summarized in Table 1. For the samples of pure sanidine, individual laser-fusion analyses of single or multiple crystal produced precise ages, with 2 sigma analytical precision typically from ± 0.25 to 0.5%. Radiogenic yields were generally high (90–100%) and K/Ca values typically ranged from 10 to 100.

Sanidine from a fall ash (sample KGJ-26) located 3 m above the fossiliferous layer gave a weighted-mean age of 10.66 ± 0.06 Ma. Biotite and hornblende from the other two sampled fall ashes (KGJ-29 and 33), both located higher in the section, gave less precise ages between 10.81 ± 0.72 Ma and 12.74 ± 0.69 Ma. The low precision of these ages probably reflects alteration of the biotite and hornblende; these minerals alter much more quickly than sanidine. Thus we consider the 10.66 ± 0.06 Ma age from sample KGJ-26 the most accurate and reliable age derived from the ash falls.

The sandstone layers (samples KGJ-24, 30, and 31) contain plagioclase and sanidine crystals of variable ages, suggesting that they were erosionally derived from a variety of older units, rather than from the syneruptive reworking of a single deposit. The ages of the youngest crystals in these samples are given in Table 1; note that these ages represent maximum ages for each layer.

As discussed above, the crossbedded sandstone immediately overlying the fossiliferous layer, represented by sample KGJ-24, was probably deposited very shortly after the fossiliferous layer. Sanidine from the sandstone yielded a maximum age of 15.85 ± 0.37 Ma. This age is considerably older than the 10.66 ± 0.06 Ma age for the overlying ash-fall (KGJ-26), but recall that the sandstone age is only a maximum age of a reworked deposit, while the ash fall age is the age of primary material. There are no signs of a depositional hiatus, such as a paleosol or an unconformity, in the section between the sampled sandstone and ash fall. Thus, 10.66 ± 0.06 Ma is taken to be the age of the Jakokkota flora.

The young maximum ages of 7.61 ± 0.30 Ma and 8.96 ± 0.54 Ma from the sandstone layers at the top of the section (KGJ-30 and 31) suggest that the stratigraphic sequence shown in Fig. 3 may have accumulated over a considerable span of time, perhaps 3 million years or more.

As for the Potosí flora, the lower bracket for its age is constrained by the Pailaviri breccia, which underlies the Caracoles tuff, and contains clasts of Agua Dulce dacite (G. Steele, pers commun.). The Agua Dulce dacite has been dated using K/Ar on biotite crystals at $20.9–21.3 \pm 0.3$ Ma (Grant *et al.,* 1979). The stratigraphic relationship between the Caracoles tuff and the sanidine-bearing ignimbrite analyzed in this study is uncertain because they are in fault contact. However, the age for the ignimbrite, 20.7 ± 0.1 Ma, is similar to the age of the Agua Dulce dacite, and is thus consistent with the ignimbrite being older than the Caracoles tuff. An upper age bracket for the Potosí flora is constrained by the 13.8 ± 0.2 Ma Cerro Rico dacite, which intrudes the fossil bearing lake beds (Francis *et al.,* 1981; Zartman and Cunningham, 1995).

COLLECTION AND DESCRIPTION

Methodology, Jakokkota flora

Berry (1922a) described a small collection of plants from Cerro Jancocata (=Jakokkota), which included a fern, a reed-like grass, and seven angiosperms, including 2 Rosaceous species and 3 legumes. All were identified to species, although in some cases the pres-

Table 1. $^{40}Ar/^{39}Ar$ Analysis for the Jakokkota and Potosí localities

Sample #*	Facies	Mineral	Age (Ma)	Error (Ma)**
Jakokkota:				
KGJ-31	X-bed sand	Plagioclase	7.61 (max.)***	0.30
KGJ-30	X-bed sand	Plagioclase	8.96 (max.)	0.54
KGJ-29	Fall ash	Hornblende	11.31	0.53
KGJ-29	Fall ash	Biotite	10.81	0.72
KGJ-33	Lapilli fall	Hornblende	12.74	0.69
KGJ-33	Lapilli fall	Biotite	11.35	0.69
KGJ-26	Fall ash	Sanidine	10.66	0.06
KGJ-24	Channel sand	Sanidine	15.85 (max.)	0.37
Potosí:				
KGP-96-6	Ignimbrite	Sanidine	20.60	0.13
KGP-96-6	Ignimbrite	Sanidine	20.57	0.09
Potosí-1	Ignimbrite	Sanidine	20.80	0.08

*See figure 3 for stratigraphy of Jakokkota samples.
**All errors are quoted at ± 2 sigma.
***The ages for the sandstone layers are the ages of the youngest crystals in the sample; these ages are thus maximum ages.

ervation of the figured specimens did not appear sufficient for identification. This collection is too small to allow paleoclimatic interpretation, so the Jakokkota flora was recollected for this study.

Over 850 leaves and leaf fragments were collected from the fossiliferous tuff and were returned to the lab. The best preserved fossils were photographed, and the venation was drawn to aid identification. Based on venation characteristics, the fossils were split into species, or more correctly for studies of fossil plants, forms, and the physiognomy, that is, morphology, of the leaves in each form was scored after the method of Wolfe (1993). Forms which had leaves which were very close in size to the next larger size category were scored in both categories in order to compensate for the size reduction observed between canopy and litter samples (Greenwood, 1992; Gregory and McIntosh, 1996). Because the primary goal of this study is climate analysis rather than systematic description, seeds and fruits were collected but not identified.

Methodology, Potosí flora

The Potosí flora, from the Cordillera Oriental (Fig. 1), was scored from the literature (Britton, 1892; Berry, 1919, 1939). Generally, scores from the literature are less representative of a flora than scores from samples collected specifically for physiognomic analysis because of "collection bias", in which especially large, well-preserved, or rare forms are preferentially collected at the expense of common taxa or fragmentary material (Taggart and Cross, 1990). A size correction was not applied to this sample because of this bias.

Another problem was that many of the 57 forms identified by Berry (1919, 1939) appeared to be identical; these were combined for a total of 35 forms. Because of these biases, the resulting physiognomic score should be viewed as preliminary; a physiognomic study of a new collection of the Potosí flora is planned for the future.

Results of sampling

The Jakokkota sample was split into 31 dicotyledonous forms (Figs 5–7), which are described in detail in the Appendix, and one fern. Of the leaves collected, 789 were sufficiently preserved that they could be identified to one of these forms.

Comparison with modern herbarium material supports Berry's identification of *Polylepis* sp. (Rosaceae). The genus, typically with compound leaves, is very common today in Andean highland habitats. At least three legumes are present in the new collection, Forms 5, 6, and 26, based on their striated pulvinuses. It is difficult to identify these forms to species only on the basis of leaves. Form 19, with prominent spinose teeth and distinctive festooned secondary and tertiary loops, is tentatively identified as *Berberis* sp., as in Form 14, with its acrodromous venation and secondary loops. Form 48 apparently corresponds to *Alnus preacuminata* of Berry (1922a), but it is unlikely that this form truly corresponds to *Alnus*, which appears from palynological data to be a recent arrival in South America (Hooghiemstra, 1989).

The two most abundant forms are *Polylepis* sp. and Form 6, a legume (Table 2). Generally, it is thought that the most abundant forms in a fossil flora represent stream-side species, but in this case, the abundance of the leaves could be due to the large number of small leaflets produced by these genera.

The physiognomic scores for the Jakokkota and Potosí samples are given in Table 3. Physiognomically, the two floras are quite similar. Note that both floras have a large percentage (70–80%) of untoothed leaves, and that the average leaf size is small, in the leptophyllous 2 size range (25–80 mm^2). No forms have leaves with elongated (attenuate) apices, but several forms have leaves with notched (emarginate) apices. The climatic significance of this distinctive physiognomy will be discussed below.

CLIMATE ANALYSIS

Foliar physiognomic method

Berry (1922a) used the nearest living relative method, or floristic method, to estimate the paleoclimate of the Jakokkota flora. In the floristic method, the nearest living relative is identified for each fossil species. The overlap of the ecological ranges of the living relatives is assumed to represent the paleoclimate.

There are problems with this method (Wolfe, 1971; Wolfe and Schorn, 1990; Chaloner and Creber, 1990). For example, no standardized method exists for matching a fossil to a modern species. In some cases, the match might be based on characters responding to climate as opposed to those with taxonomic significance. After the match is made, the assumptions are made that the fossil species evolved into the modern species, and that the ecological tolerance of the genera did not change with time, neither of which is necessarily true.

In this study, the foliar physiognomic method of Wolfe (1993, 1995) is used to estimate paleoclimate. This method is based on the observation that the leaf physiognomy, that is morphology, of woody dicotyledons varies with climate. For example, the percentage of entire, that is, smooth-margined, species tends to increase with the mean annual temperature (Wolfe, 1979). Leaf size and leaf width tend to be smaller in sunny/dry environments and larger in shady/moist environments (Webb, 1968; Givnish, 1979, 1984; Wolfe,

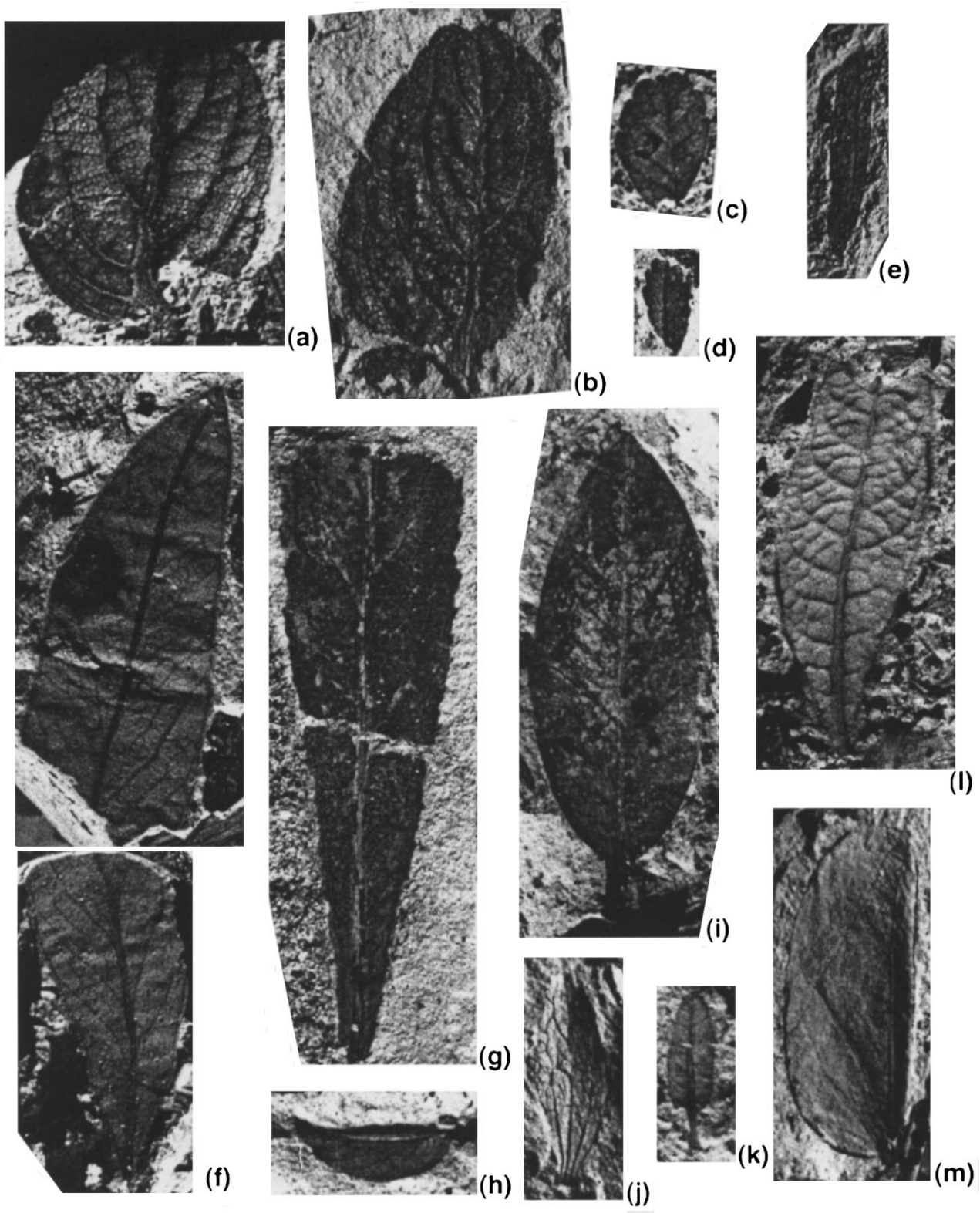

Fig. 5. Photos of leaf forms, ×4 except where noted. (a) Form 1, specimen 96.22 (×5). (b) Form 1, specimen 96.1. (c) *Polylepis* sp., specimen 96.198. (d) *Polylepis* sp., specimen 96.432. (e) Form 6 (legume 2), specimen 96.329. (f) Form 4, specimens 96.159 a and b. (g) Form 8, specimen 96.30. (h) Form 10, specimen 96.70. (i) Form 12, specimen 96.40. (j) Form 14 (*Berberis*), specimen 96.215. (k) Form 17, specimen 96.142. (l) Form 3, specimen 96.7. (m) Form 5 (legume 1), specimen 96.441.

1993), and leaves in very wet environments often have elongated apices, or "drip-tips", which allow excess water to be removed (Dean and Smith, 1979), while leaves in dry climates tend to have notched, or emarginate, apices (Gregory, 1994).

These relationships between leaf physiognomy and climate exist because leaves influence heat exchange with the atmosphere, transpiration, photosynthesis, and nutrient supply (Taylor, 1975; Givnish, 1979, 1987). Thus the leaf physiognomy of a plant affects its

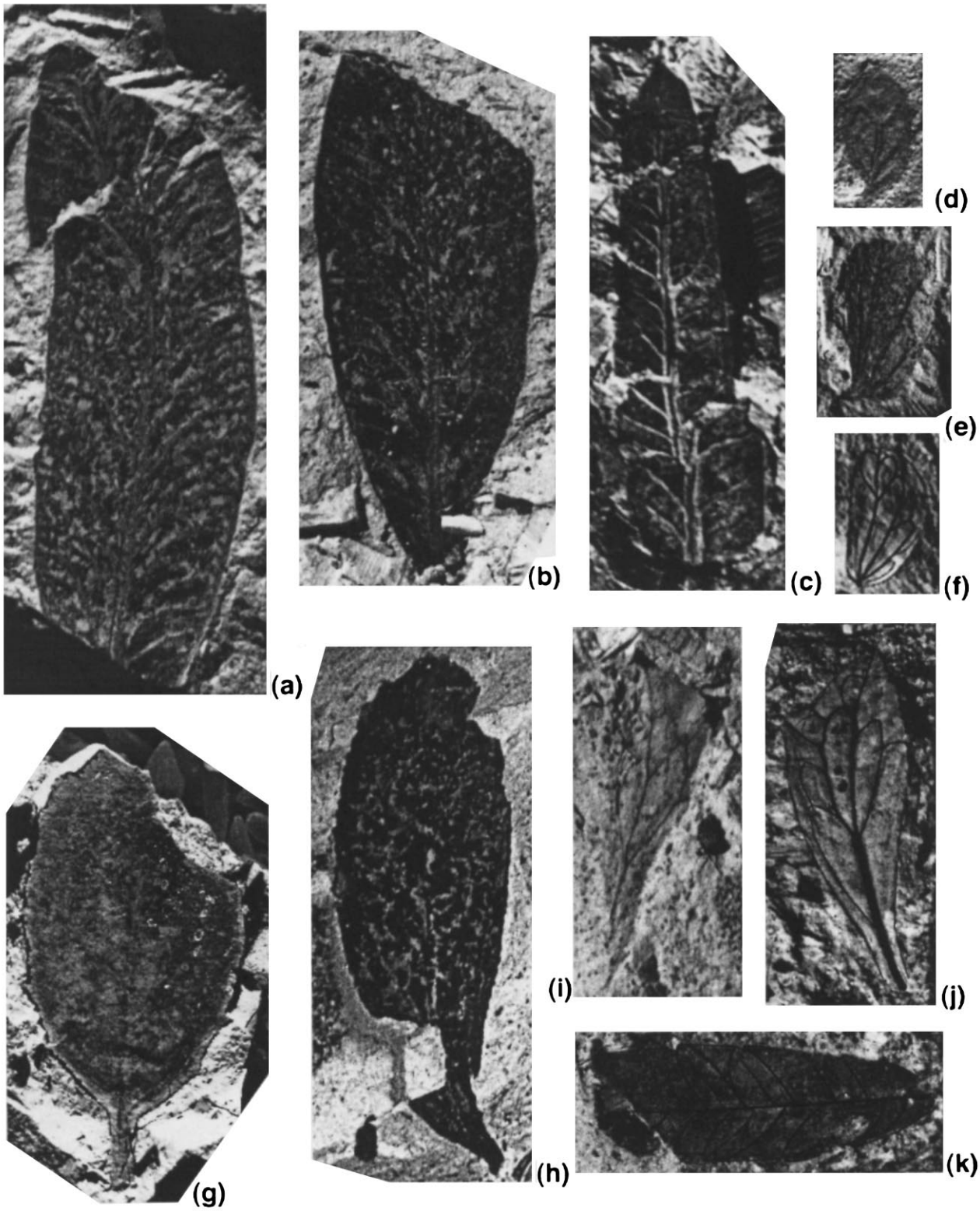

Fig. 6. Photos of leaf forms, ×4 except where noted. (a) Form 13, specimen 96.236a. (b) Form 13, specimen 96.236b. (c) Form 11, specimen 96.205. (d) Form 18, specimen 96.143. (e) Form 26 (legume 3), specimen 96.279 (×5). (f) Form 26 (legume 3), specimen 96.451. (g) Form 9, specimen 96.31 (×3). (h) Form 22, specimen 96.260. (i) Form 19 (*Berberis*), specimen 96.171. (j) Form 19 (*Berberis*), specimen 96.238. (k) Form 28, specimen 96.286.

efficiency in a given environment. Such physiological responses to climate are thought to be less subject to evolutionary changes than the ecological tolerances of genera, which are used in the nearest living relative method of estimating paleoclimate.

Both univariate and multivariate analyses have been used to estimate mean annual temperature (MAT) from leaf physiognomy (i.e. Wing and Greenwood, 1993; Wolfe, 1995; Gregory and McIntosh, 1996; Wilf, 1997; Wiemann *et al.,* in preparation). Leaf margin

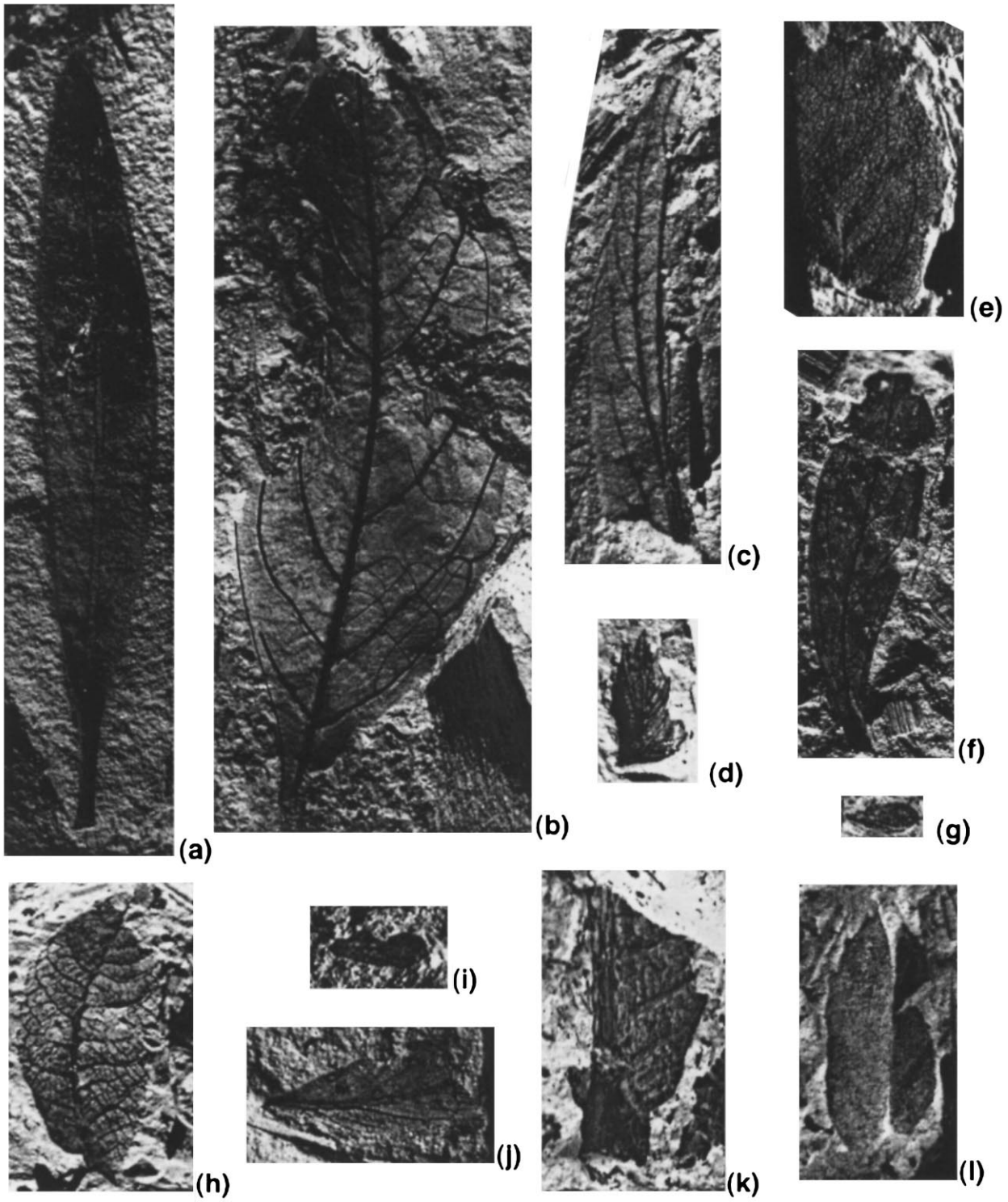

Fig. 7. Photos of leaf forms, ×4 except where noted. (a) Form 33, specimen 96.334. (b) Form 25, specimen 96.339. (c) Form 43, specimen 96.98. (d) Form 40, specimen 96.461. (e) Form 46, specimen 96.261. (f) Form 47, specimen 96.237. (g) Form 41, specimen 96.474 (×2.5). (h) Form 50, specimen 96.455. (i) Form 30, specimen 96.80. (j) Form 49, specimen 96.216. (k) Form 48, specimen 96.487. (l) Form 45, specimen 96.226.

analysis (LMA), a univariate technique, uses the observed linear relationship between MAT and the percent entire margined species (Fig. 8). Multivariate analyses use the Climate-Leaf Analysis Multivariate Program (CLAMP) database of Wolfe (1995), the latest version of which includes scores for 31 leaf physiognomic character states from 141 modern vegetation sites from North America (including Mexico), the Caribbean, Fiji, New Caledonia, and Japan. Multiple regression analysis of the CLAMP database assumes that the character states have linear relationships with climate, while the CLAMP technique of Wolfe (1995), which uses canonical correspondence analysis, allows for non-linear relationships.

Table 2. Abundance of different leaf forms for the Jakokkota flora

FORM	# sp.	%
2	244	30.9
6	216	27.4
11	67	8.5
47	32	4.1
13	26	3.3
1	22	2.8
14	21	2.7
8	19	2.4
22	15	1.9
10	14	1.8
26	12	1.5
41	11	1.4
5	10	1.3
19	10	1.3
17	9	1.1
18	8	1.0
12	7	0.9
4	6	0.8
25	6	0.8
46	6	0.8
28	4	0.5
40	4	0.5
43	4	0.5
30	3	0.4
33	3	0.4
3	2	0.3
9	2	0.3
45	2	0.3
49	2	0.3
48	1	0.1
50	1	0.1
TOTAL	789	

sp. = number of specimens.

A controversy exists over which method derives the best estimates of MAT (Wolfe, 1995; Wilf, 1997; Wiemann *et al.,* in preparation). The purpose of this paper is not to provide a rigorous statistical evaluation of the various methods, however, it is important for this study to assess which methods derive the most accurate results. In order to compare the methods, the residuals were calculated for each model, LMA, MRA, and CLAMP (Table 4) using the same database, the CLAMP 3B database of Wolfe (1995), which is the most extensive physiognomic database available. The residuals are the differences between the MAT values for each site predicted by the model and the observed MAT values.

The results of this analysis suggest that the multivariate techniques are more successful at predicting temperature than LMA (Table 4), because their average residuals are lower, and fewer sites have errors over 2°C. The two multivariate techniques have very similar average residuals, and a similar number of sites with errors less than 2°C. From a philosophical standpoint, CLAMP analysis is preferable to MRA analysis because it can handle both linear and non-linear relationships between physiognomic character states and climate (Wolfe, 1995). However, results from other analyses suggest that LMA is most successful at predicting mean annual temperature (Wilf, 1997).

For comparison, all methods were used to estimate the mean annual temperature of the Jakokkota and Potosí floras. The CLAMP method as described by Wolfe (1995) and Wolfe *et al.* (1996) was used to derive estimates of other climate variables such as mean growing season precipitation and enthalpy. Plots of CLAMP axis 1 (temperature) and axis 2 (water-stress) scores for the fossil vegetation were compared with

Table 3. Physiognomic character state scores for the Jakokkota and Potosí floras

LPCS*	Jakokkota score (%)	Potosí score (%)	LPCS	Jakokkota score (%)	Potosí score (%)
1. TLob	1.7	5.7	8. AEmg	4.0	17.7
2. NoT	70.0	80.0	9. APEX: ARnd	54.0	55.9
3. TRg	18.3	11.4	AAct	46.0	44.1
4. TCl	8.3	7.1	AAtn	0.0	0.0
5. TRnd	16.7	7.1	10. BASE: BCd	1.2	2.5
5. TAct	16.7	12.9	BRnd	28.0	42.2
6. TCmp	0.0	0.0	BAct	70.8	55.4
7. SIZE: Nan	7.8	5.7	11. L:W: LW < 1	0.0	0.0
Le1	14.5	13.6	LW1-2	21.1	23.8
Le2	32.8	35	LW2-3	40.6	23.3
Mi1	38.7	23.6	L:W3-4:1	20.6	20.3
Mi2	6.2	16.4	L:W > 4:1	17.8	32.6
Mi3	0.0	5.7	12. SHAPE: SOb	19.4	14.7
Me1	0.0	0.0	SElP	64.4	73.5
Me1	0.0	0.0	SOv	16.1	11.8
Me3	0.0	0.0			

*Numbers (1., 2., etc.) denote categories. Some categories have only two character states, for example 'Lobed' and 'Not Lobed' are in the category 'Lobed'. For simplicity, only one character state is usually reported. 'Teeth Acute' and 'Teeth Round' are an exception, as both are reported. Other categories, such as size, contain several character states and all are reported. Quantification of physiognomic score for given leaf from: 1) if present, character state receives score of 1 divided by number of character states present for form in that category; 2) if absent, character scored 0; 3) if partly present, scored as 0.5 divided by number of character states in category. Form scores then added for each character state and divided by total number of forms to derive physiognomic score. See Wolfe (1993) for details of scoring and definitions. ABBREVIATIONS: LPCS: Leaf Physiognomic character state, TLob = Teeth lobed, NoT = No teeth, TRg = Teeth regularly spaced, TCl = Teeth closely spaced, TRnd = Teeth round, TAct = Teeth Acute, TCmp = Teeth compound, Le1,2 = Leptophyllous1,2; Mi1,2,3 = Microphyllous 1,23; Me1,2 = Mesophyllous 1,2; AEmg = Apex emarginate, ARnd = Apex Round, AAct = Apex acute, AAtn = Apex attenuate, BCd = Base cordate, BRnd = Base round, BAct = Base acute, L:W = Length to width ratio, Sob = Shape obovate, SElp = Shape elliptical, SOv = Shape Ovate

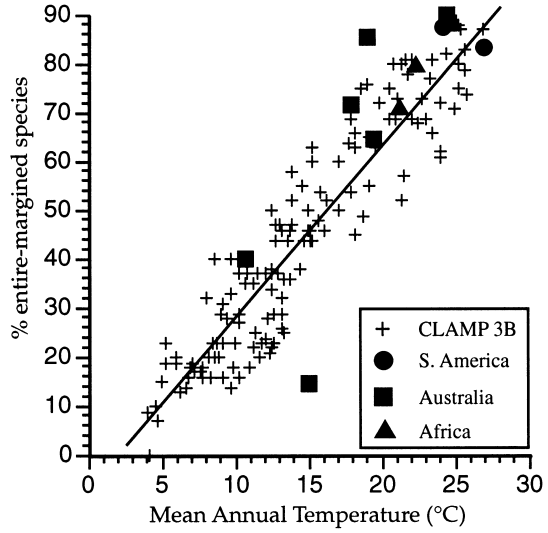

Fig. 8. Mean annual temperature versus percent entire-margined species for the CLAMP 3B modern vegetation dataset of Wolfe (1995) (pluses). Sites from Peru and Bolivia (circles; Wilf, 1997), Australia (squares; Greenwood, 1992); and Africa (triangles; Jacobs and Deino, 1996) are plotted for comparison. The regression line is for the CLAMP 3B dataset and has an r^2 of 87%.

scores for the modern samples, in order to determine the most similar modern flora (Wolfe, 1995).

Sources of error

The standard errors for the CLAMP analyses are given in Table 5; these are the average formal errors calculated from the residuals. Wilf (1997) shows that for samples of less than about 75 species, the error associated with using a small sample to represent a large flora is greater than the average formal error, and is thus a better approximation of the actual error. Using the equation of Wilf (1997), the sampling error for the Jakokkota flora with 31 species is 2.5°C and for the Potosí flora with 35 species is 2.1°C.

Other errors are associated with taphonomic factors, that is, processes associated with transportation, deposition, and fossilization of leaves. Samples in the CLAMP 3B database were collected from the canopies of living trees, while fossil deposits represent samples of leaf litter. Studies by Greenwood (1992) and Roth and Dilcher (1978) suggest that there is a reduction in leaf size between canopy samples and litter samples deposited on the ground or in lakes; any stream transportation of the leaves increases this bias. As mentioned in the methods section above, a size correction was applied to the Jakokkota sample to correct for this bias.

Roth and Dilcher (1978) suggest that there also might be a reduction in the number of entire-margined species from canopy to litter samples. However, their sample size was very small; more studies are needed to confirm their observations. Comparison of litter and canopy-derived CLAMP samples from the same site suggest that the physiognomic differences between them, which were not detailed, translate into differences of ±0.2–0.7°C in MAT estimates (Wolfe, 1993). Taphonomic sources of error are discussed in more detail in Gregory and McIntosh (1996).

Another possible source of error is changing levels of atmospheric CO_2. Increased CO_2 levels appear to increase the water-use efficiency of plants, and thus could potentially effect their leaf physiognomy. However, paleoatmospheric studies suggest that Miocene CO_2 levels were similar to, or only slightly higher than modern CO_2 levels (Cerling, 1991; Van Der Burgh *et al.,* 1993). Preliminary results from growth chamber experiments suggest that such a small increase of CO_2 would not have a significant effect on leaf physiognomy (Gregory, 1996).

The most serious problem for this study is the lack of physiognomic data for Southern Hemisphere floras. Wolfe (1979) notes that vegetation from the Southern Hemisphere tends to have a higher percentage of entire-margined species for a given temperature than vegetation from the Northern Hemisphere, perhaps because of the lack of development of broad-leaved deciduous forests in the south. Thus, using a Northern Hemisphere database might give results for Southern Hemisphere floras which are too warm.

This bias appears to be less evident for paratropical (MAT = 20–25°C) and tropical (MAT > 25°C) floras (J. Wolfe, personal communication, 1997); for example, leaf margin versus MAT data for tropical and paratropical sites from Peru and Bolivia (Wilf, 1997), Africa (Jacobs and Deino, 1996), and Australia (Greenwood, 1992) are not significantly different from data in the CLAMP 3B database (Fig. 8).

A study by Jordan (1997) on modern vegetation from Australia and New Zealand found that the CLAMP method greatly overpredicted the MAT of the sample sites. However, it is unclear whether the bias resulted from physiognomic factors or from other factors, such as the poor soils, or the interpolated climate data. Estimating MAT from several databases from various geographic regions can help address this problem, but resolution of this question awaits the

Table 4. Statistical evaluation of the various physiognomic models:

Statistic	LMA	MRA	CLAMP
Average value of residual (°C)	1.8	1.5	1.6
# residuals 0–1 °C*	48	60	55
# residuals 1–2 °C	38	39	42
# residuals 2–3 °C	30	25	24
# residuals 3–4 °C	16	15	17
# residuals 4–5 °C	8	2	2
# residuals 5–6 °C	1	0	1
# residuals < 2 °C	86	99	97
# residuals > 2 °C	55	42	44

*number of residuals between the given temperature range. LMA = Leaf margin analysis. MRA = Multiple Regression Analysis. CLAMP = Climate Leaf Analysis Multivariate Program (correspondence analysis).

Table 5. MAT estimates for the Jakokkota and Potosí floras using the various physiognomic models

Database and Method	N	Error (± °C)	MAT (°C)	MAT (°C)
Leaf Margin Analysis			**Jakokkota**	**Potosí**
Australia[1]	8	3.3	~19.5	~22
Southern Hemisphere[2]	?	?	~20	~22.5–23
Western Hemisphere[3]	9	2.0	22.3	25.1
Eastern Asia[4]	34	1.0	22.6	25.6
Northern Hemisphere (CLAMP 3B)[5]	141	2.2	21.0	23.5
Multivariate analysis:				
MRA, CLAMP 3B database[6]	141	1.9	18.6	21.5
CLAMP; CLAMP 3B database[7]	141	1.9	21.0	21.7

1. extrapolated from Fig. 12 Greenwood (1992). 2. Wolfe (1979), p. 34, and Wolfe and Upchurch (1987). 3. Wilf (1997). 4. Wolfe (1979). 5. Calculated in this study from the CLAMP 3B database, MAT = (24.96*NoT/100) + 3.54. 6. Calculated in this study from the CLAMP 3B database: MAT = (18.43*NoT/100) – (17.39*LW < 1/100) + (8.17*AEmg/100) + (4.33*AAtn/100) + 5.35. 7. Wolfe (1995). N = the number of samples in the database.

collection of CLAMP samples from the Southern Hemisphere.

Results and discussion of climate analysis

The results of LMA, MRA, and CLAMP analysis for the Jakokkota and Potosí floras suggest that subtropical-dry or paratropical-dry conditions existed in the Miocene. MAT estimates for Jakokkota range from 18.6° to 22.6°C and for Potosí from 21.5° to 25.6°C (Table 5). The cooler estimates are derived from the CLAMP 3B and Southern Hemisphere datasets, with the coolest estimates from MRA analysis. The warmest temperatures are derived from the East Asian dataset. Within each model, the Potosí flora is estimated to be warmer than the younger Jakokkota flora.

Of these results, we favor those from multivariate analysis. As discussed above, our analysis of residuals suggests multivariate analyses are more successful in predicting MAT for modern sites than univariate analysis (LMA). Also, the multivariate models, as of now, are based on larger datasets than LMA. Another reason to favor the multivariate analyses is that they derive the most conservative MAT estimates. By conservative we mean that they imply the least amount of temperature and thus elevation change between the Miocene and the present. Multivariate analysis implies a MAT of 18.6–21.0 ± 2.5°C for Jakokkota and 21.5–21.7 ± 2.1°C for Potosí.

Comparison of these MATs to modern climate data (Table 6) suggests that the Miocene Altiplano–Cordillera Oriental area was 10–13°C warmer than today. Also, CLAMP analysis suggests that the Miocene growing season length, defined as the number of months with a mean monthly temperature greater than 10°C, was 10.6–10.8 ± 2.0 months for both floras, compared to only 2–3 months today.

Precipitation during the growing season for both floras is estimated to have been on the order of 50 ± 43 cm, implying that the climate was paratropical dry, rather than paratropical wet. This hypothesis is supported by the location of Jakokkota and Potosí on plots of CLAMP 1st and 2nd axis scores, indicating that the fossil floras are most similar to modern floras in the database from the thorn scrub of northern Mexico and from dry areas of Puerto Rico, as plotted by Wolfe (1995).

The error on the estimates of precipitation is large, thus one cannot evaluate whether the fossil sites were wetter or drier in the Miocene than today. Presently, Jakokkota and Potosí have a mean annual precipitation of 31 and 44 cm, respectively (Vose *et al.,* 1992).

Determining the precipitation regime is of interest to paleoelevation studies, because the present day aridity of the Altiplano is due in a large part to the Andean Cordillera. The Andes create a rain shadow which blocks moisture from the Amazon Basin, and they stabilize the South Pacific subtropical anticyclone off the western coast of South America (Alpers and Brimhall, 1988). This pressure system drives upwelling along the coast and the Peru Current (or Humboldt Current), which transports cooler waters from the south along the coast. The air on the east flank of the South Pacific anticyclone descends along the coast, and picks up little moisture from the cold surface waters (Alpers and Brimhall, 1988).

Table 6. CLAMP-derived climate estimates and modern values

Climate variable	Jakokkota		Potosí	
MAT (°C)	18.6–21.0	*8.3*	21.5–21.7	*~8.6*
WMMT (°C)	30.4	*11.4*	30.4	*~10*
Enthalpy (kJ/kg)	317.9	*?*	319.1	*?*
GSL (months)	10.6	*3*	10.8	*~2*
MGSP (cm)	49.8	*15.1*	47.4	*5.4*
MAP (cm)	?	*30.7*	?	*44.1*
MMGSP (cm)	4.1	*5.1*	3.9	*2.7*
3WM (cm)	30.0	*15.1*	28.9	*14.9*
3DM (cm)	40.5	*0.5*	43.3	*0.4*
RH (%)	55.3	*?*	54.4	*?*

Modern climate data (in italics) calculated from monthly average data of Vose *et al.* (1992). Jakokkota data from the Charaña station (4059 m), 60 km to the south-west. Potosí temperature data from the Sucre station (2903 m), 80 km to the northeast. Sucre has a MAT of 15.7°C; if we apply the global lapse rate of 0.59°C 100 m^{-1} (see text), then Potosí has a MAT ~8.6°C. Precipitation data from Potosí station. MAT = mean annual temperature, standard error (s.e.) = 1.9°C. WMMT = warm month mean temperature, s.e. = 2.7°C. Enthalpy, s.e. = 5.6 kJ/kg. GSL = growing season length, s.e. = 2.0 months. MGSP = Growing season precipitation (the growing season is defined as the number of months with a mean monthly temperature > 10°C), s.e. = 42.9 cm. MMGSP = mean monthly growing season precipitation, s.e. = 2.3 cm. 3WM = total precipitation of 3 consecutive wettest months, s.e. = 20.7 cm. 3DM = total precipitation of 3 driest months, s.e. = 20 cm. RH = Relative humidity, s.e. = 12.3%.

Based on the development of porphyry-copper deposits in the Atacama Desert, Alpers and Brimhall (1988) argue that climate conditions changed from arid-semiarid to hyperarid in the Atacama desert, located to the west of the Altiplano in northern Chile (Fig. 1) at approximately 15 Ma. This drying trend is not evident in the botanically estimated precipitation data, either because (1) it did not occur, (2) it did occur, but the Potosí flora is younger than 15 Ma and thus post-dates the drying, or (3) it did occur, but is obscured by the large errors on the estimates.

ELEVATION ANALYSIS

Tectonic history of the Andes

The paleoclimate estimates for the Jakokkota and Potosí floras can be used to estimate the elevations at which they grew, because several climatic factors vary with climate. Such paleoelevation estimates are of interest because the Miocene was an important era in the tectonic history of the Andes, summarized here briefly.

The first evidence of Andean deformation, a transition from platform deposits to westerly derived foreland deposits, appears in the late Cretaceous (Coney and Evenchick, 1994), specifically 89 Ma in Bolivia (Sempere *et al.,* 1997). Subduction existed prior to this time, but apparently was not accompanied by extensive orogenesis. Several workers have proposed that the onset of compression was triggered by the initiation of spreading in the South Atlantic 110–130 Ma (Coney and Evenchick, 1994; Russo and Silver, 1996).

The Andean orogeny is, in general, similar to the Cordilleran Orogeny of the North American Cordillera, though due to earlier initiation of spreading in the North Atlantic (~170 Ma), the timing of tectonic and sedimentary events in the south lag those in the north by about 50–60 Ma (Coney and Evenchick, 1994). Thus, the modern Andes are often viewed as an analog of the Cretaceous–early Cenozoic North American Cordillera.

In Bolivia, compression created a fold-thrust belt and foreland basin system, and this system continuously migrated eastward during the orogeny. For example, in the late Cretaceous to Paleocene, a succession of marginal marine and lacustrine sediments were deposited in the area which now comprises the Altiplano to Subandean zones. These deposits are interpreted as back-bulge deposits, or the easternmost deposits in the foreland basin system (Horton and DeCelles, 1997; Sempere *et al.,* 1997). These deposits are critical to study of the uplift history, because they are only non-controversial paleoelevation datum. They indicate that the Central Andes were at sea level until at least 60 Ma (Sempere *et al.,* 1997).

In the Eocene, the system migrated to the east, and the foredeep now occupied the area of the Altiplano and eastern Cordillera, the forebulge the eastern Cordillera Occidental (Horton and DeCelles, 1997).

In the late Oligocene, around 27 Ma, the foreland system again migrated to the east, to occupy the Subandean zone, and the Altiplano and eastern Cordillera Oriental underwent significant deformation as part of the fold- and thrust belt (Sempere *et al.,* 1990). This deformation lasted until ~9–10 Ma (Allmendinger *et al.,* 1977). At that time, deformation again shifted to the east; compression ceased in the Altiplano and Cordillera Oriental, and commenced in the Subandean zone between 6–10 Ma.

Models of Andean deformation

Today the average crustal thickness of the Altiplano is 60–65 km, as calculated by broadband seismic studies (Beck *et al.,* 1996; Zandt *et al.,* 1996), which is considerably thicker than "standard" continental crust of 30–35 km. Most recent tectonic models suggest that uplift was primarily due to crustal thickening from crustal shortening (i.e., Sheffels, 1990; Allmendinger *et al.,* 1997; Lamb *et al.,* 1997; Okaya *et al.,* 1997), and that it occurred during the time of maximum shortening. These models are summarized below:

(1) Molnar and Lyon-Caen (1988) suggest that mountains have a maximum sustainable elevation or crustal thickness, which is related to plate tectonic forces. When this limit is reached, the range then starts to build laterally in width, creating a high plateau. This model thus suggests that the Altiplano reached its present elevation, a critical height, by ~10 Ma (Fig. 9). Recall that at this time, surface deformation

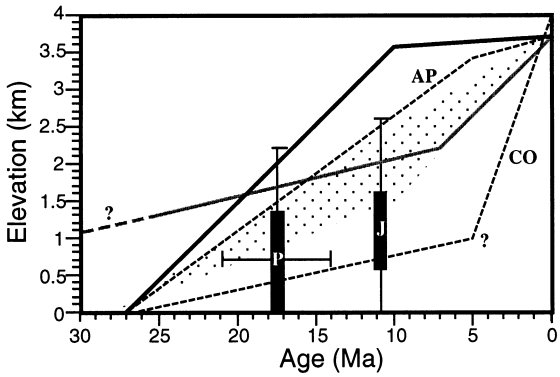

Fig. 9. Andean uplift histories from various lines of evidence. Black bars with letters and error bars = Jakokkota (J) and Potosí (P) elevation estimates, this study. Thick black solid line = critical elevation model of Molnar and Lyon-Caen (1988). Dotted trapezoid = two phase model of Gubbels et al. (1993). Gray line = modified two phase model of Lamb et al. (1997). Thin black dashed lines = modified two phase model of Okaya et al. (1997); AP = Altiplano, CO = Cordillera Oriental.

ceased in the Altiplano and Cordillera Occidental and migrated to the east.

(2) In contrast, the two-stage model of Isacks (1988), updated by Gubbels *et al.* (1993) and Allmendinger *et al.* (1977), suggests that the eastward migration of active thrusting at ~10 Ma occurred before the Altiplano reached its present height. They estimate that compressional deformation in the Altiplano and Cordillera Oriental from ~25–10 Ma created intermediate elevations, around 1500–2500 m (Gubbels *et al.,* 1993). Then, from ~10 Ma to the present, upper crustal shortening ceased as the Cordillera Oriental overthrust the craton, causing shortening of the lower crust of the Altiplano and Cordillera Oriental and thus additional uplift (Fig. 9).

(3) The tectonic model of Lamb and Hoke (1997) and Lamb *et al.* (1997) differs from the above model in that it includes significant deformation before the late Oligocene; it predicts ~1300 m of elevation by 25 Ma based on estimates of surface shortening (Fig. 9). Their estimate of 2200 m of elevation at 7 Ma is based on paleoelevation estimates from fission track data and geomorphologic surfaces, which are problematic (England and Molnar, 1990; Chase *et al.,* 1998), and river gradient studies. The model suggests that the uplift since 7 Ma was created by lower crustal shortening, as proposed by the above model, and/or delamination of the basal part of the lithosphere.

(4) Okaya *et al.* (1997) propose that the Altiplano and Cordillera Occidental underwent different uplift histories. From 27 to 5 Ma the lower crust under the Cordillera Oriental underthrust the Altiplano, uplifting it to 3400 m while creating only minor elevation in the Cordillera Oriental (Fig. 9). Then from 5 Ma to the present, the Subandes thrust beneath the Cordillera Oriental, creating the elevation profile observed today.

Because each of these models implies a distinct uplift history (Fig. 9), they can be assessed by estimating the paleoelevations of the Jakokkota and Potosí floras.

Methodology: botanically-based paleoaltimeters

As of now, there are two botanically-based paleoaltimeters; both use the fact that certain climate parameters vary with elevation. One method uses botanically-based estimates of enthalpy (Forest *et al.,* 1998), the other uses botanically-based estimates of mean annual temperature (MAT) (Meyer, 1992; Wolfe, 1992). Though the resulting estimates generally have large errors (700–1000 m), if enough floras are studied a reasonable uplift history can be reconstructed (i.e., Wolfe *et al.,* 1997; Chase *et al.,* 1998). These two methods are summarized below:

Enthalpy-based paleoaltimeter. The paleoaltimeter developed by Forest *et al.* (1998, in press) is based on the longitudinal and altitudinal invariance of moist static energy of airmasses at mid-latitudes on greater than annual timescales. Moist static energy, written h, is the total energy content of moist air not including kinetic energy (which is negligible) and is defined as:

$$h = H + gZ \tag{1}$$

where H is moist enthalpy, which is a function of temperature and relative and specific humidity, g is the gravitational acceleration, and Z is altitude. The moist enthalpy can be further defined as the change in energy at a constant pressure and divided into specific heat and latent heat energies:

$$H = c'_{\mathrm{p}}T + L_{\mathrm{v}}q \tag{2}$$

where c'_{p} is the specific heat capacity of moist air, T is temperature, L_{v} is the latent heat of vaporization, and q is the specific humidity.

The invariance of moist static energy with longitude and altitude arises from the interaction between the atmospheric general circulation and atmospheric convection. Convection acts to mix air vertically whereas the general circulation tends to transport and mix along the direction of the mean wind. The resulting interaction implies that conserved thermodynamic properties of the air, like moist static energy, tend to reflect the upper air wind pattern at the surface (see Forest *et al.* (1998) for an in depth discussion). Forest *et al.* (1998) have examined mean annual moist static energy for North America between 30 and 60°N, where the winds are predominantly westerly, and quantified the error associated with assuming that this variable is invariant with longitude.

To estimate a paleoaltitude for a flora between 30–60°N, one assumes that the coeval sea-level moist static energy can be calculated from an estimate of sea level enthalpy, which can be estimated from a fossil flora using the CLAMP method, and that moist static energy is invariant with longitude. One then estimates the enthalpy of the inland flora, and from equation (1), the elevation can be estimated after:

$$Z = \frac{H_{\text{sea level}} - H_{\text{high}}}{g} \tag{3}$$

where sea level and high indicate the two independent enthalpy estimates. Here, we have assumed that sea level is known from some independent indicator such as sediments or other fossils.

While this method has been verified for the North American present-day climate, no similar estimate has been attempted for Bolivia. Because of the seasonal variation in circulation over South America, similar to monsoonal circulation (Meehl, 1992), the application of the enthalpy-based paleoaltimeter to this area is likely to be difficult. In the southern summer, convection over the Altiplano draws in warm, moist

air from the Amazon Basin to the northeast. In the southern winter, cool, dry air arrives from the Antarctic to the south, or the Pacific Ocean to the west (Johnson, 1976). Thus it is likely that moist static energy values for the Bolivian Altiplano vary seasonally, according to whether the air parcels derive from the Amazon Basin–Atlantic ocean, or from the Pacific–Antarctic Oceans. Waters on the west coast of South America are considerably colder than on the east coast because of the Peru Current, the cold water current which flows from south to north along the coast, so the sea-level enthalpy of air derived from the Pacific or Antarctic Ocean would be significantly less than the sea-level enthalpy of air derived from the Atlantic Ocean–Amazon Basin (C. Forest, personal communication).

An additional complication is that this quasi-monsoonal circulation was most likely greatly enhanced by Andean uplift. Thus, one needs to know the elevation to estimate paleocirculation patterns. Therefore as of now, it is not possible to use the enthalpy paleoaltimeter for Bolivian floras.

MAT-based paleoaltimeter. The basis for the mean annual temperature (MAT)-based altimeter is the observation that temperature decreases with elevation. In a column of free air, the lapse rate, that is the temperature decline with altitude, is $0.6^{\circ}C\ 100\ m^{-1}$. The relationship is more complicated over land, because the heating of air is affected by the nature of the ground surface (Meyer, 1986).

To estimate the paleoelevation, Z, of a fossil flora, one compares the paleoMAT of the flora with the paleoMAT of a coeval flora which grew near sea level then applies a "terrestrial lapse rate" after the equation of Axelrod and Bailey (1976):

$$Z = \frac{MAT_c - MAT_i}{\gamma} + S \qquad (4)$$

where MAT_c = mean annual temperature at sea level (°C); MAT_i = MAT from a coeval inland site (°C); γ = "the empirical relationship between mean annual temperature at the surface and altitude" (Forest *et al.,* 1995), equivalent to the terrestrial lapse rate of Wolfe (1992) and Meyer (1986, 1992) and S = ancient sea level relative to modern sea level (m).

As in the enthalpy-based method, a fossil flora that grew at or near sea level is chosen for comparison with the inland flora, because sea level is the only paleoelevation which can be identified with certainty in the geologic record. Unfortunately, no Miocene sea-level floras from Bolivia have been studied, so there is no coeval flora which can be used for comparison with the Jakokkota and Potosí floras. We can only compare the paleoclimate of these floras with the modern climate at the same location to get some idea of the paleoelevation.

The problem with this approach of comparing the ancient and modern climates is that the temperature difference between them is a combination of climate change due to uplift, global climate change, latitudinal continental drift, and changes in paleogeography. Thus, one is presented with the difficult tasks of extricating the various climate signals, modifying equation (4) to derive:

$$Z = Z_m - \left(\frac{MAT_i + \Delta MAT_{gc} + \Delta MAT_{cd} + \Delta MAT_{pg} - MAT_m}{\gamma}\right) + S \qquad (5)$$

where Z_m = the modern elevation; ΔMAT_{gc} = the change in MAT since deposition of the fossil flora due to global climate change; ΔMAT_{cd} = the change in MAT since the deposition of the fossil flora due to latitudinal continental drift; ΔMAT_{pg} = the change in MAT since the deposition of the fossil flora due to changes in paleogeography; and MAT_m = the modern MAT.

An important factor to subtract out is ΔMAT_{gc}, or global climate change since the deposition of the floras. Not enough studies of fossil floras have been undertaken to estimate the terrestrial temperature change in the tropics, but it is possible to estimate the magnitude of temperature change in the tropical oceans from stable isotope studies of marine microorganisms.

In terms of temperature, the late Miocene ocean appears to have been similar to the modern ocean. Oxygen isotope data from planktic foraminifera from DSDP sites in the western equatorial Pacific suggest that low-latitude surface waters cooled approximately 0–1°C since the Jakokkota flora was deposited (Savin *et al.,* 1975; Savin, 1977); the generalized curve based on these sites and additional sites from the north Pacific suggest closer to no change in tropical temperature. Oxygen isotope analyses from the time-slice study of Savin *et al.* (1985) suggest that surface temperatures in the equatorial Pacific warmed slightly since 8 Ma, perhaps a degree, while temperatures in the Miocene equatorial Atlantic were similar to modern values. Thus, it appears that there was little change in ocean surface temperatures in the mid-ocean from the time of the Jakokkota flora to the present, though these estimates are complicated by the assumptions about ice volume, and the depth at which the organisms lived.

Analysis of diatoms and diatomites suggest that the Peru Current has existed for at least the last 40 Ma, and that it intensified during the late Miocene (Barron, 1984; Dunbar *et al.,* 1990), either during or after the deposition of the Jakokkota flora. Intensification of the Peru Current would decrease sea surface temperatures along the west coast of South America. Changes in the Peru Current probably did not have a large affect on temperatures in the Altiplano area; modern climate data suggests that the

current only influences about a 100-km wide strip along the coast and the lower west slopes of the Andes (Fig. 10) (Johnson, 1976). The Jakokkota and Potosí floras are located 175 and 450 km inland, respectively.

It is more difficult to estimate global temperature change since deposition of the Potosí flora than the Jakokkota flora because of the uncertainty in the age of the Potosí flora. The generalized low-latitude surface temperature curve of Savin *et al.* (1975) suggests that from 20.7–13.8 Ma to the present, temperatures were as much as 6°C cooler than today, or 1°C warmer.

Some workers contest the ice volume assumptions made to calculate these temperatures, and argue that the tropics maintain a fairly constant temperature through time (Matthews and Poore, 1980). However, oxygen isotope analysis of corals from Barbados suggests that the tropical oceans cooled significantly (5°C) during the Last Glacial Maximum (Guilderson *et al.,* 1994), which indicates that the tropical oceans probably do not maintain a constant temperature.

In terms of the ΔMAT_{cd}, or the change in temperature due to latitudinal continental drift, the area of the Bolivian Altiplano was ~2° latitude further south 10 Ma, and ~3.5° latitude further south 20 Ma (Smith *et al.,* 1981). Stable isotope data suggest that the late Miocene latitudinal gradient was about 3/4 of the modern-day gradient (Loutit *et al.,* 1983). Thus if we take the modern temperature gradient in the eastern lowlands of Bolivia and Argentina of 0.44°C° latitude

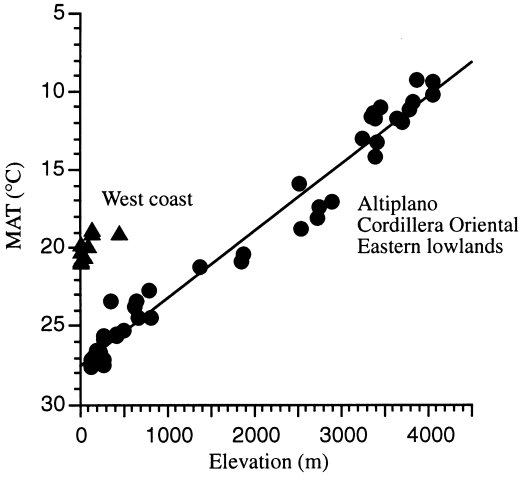

Fig. 10. Mean annual temperature (MAT) and elevation data for climate stations between 9° and 23° latitude S. Data from the west coast and western slope in triangles, data from the Altiplano, eastern slope, and eastern lowlands in circles (see Fig. 1 for physiographic provinces). In order to compensate for MAT variation with latitude, MAT data was projected to 9° latitude S using the observed rate of change of 0.134°C/° latitude in the eastern lowlands data. Regression equation MAT = −0.00431*Elevation (m) + 27.5. $r^2 = 97.1$, $F = 1374$. Climate data from Vose *et al.* (1992) and Ronchail (1985).

(Fig. 10), and reduce this by 3/4 to 0.33°C° latitude^{-1} to simulate the Miocene, the area would have warmed 0.7°C since the Jakokkota flora was deposited 10 Ma, and 0.9–1.2°C since the Potosí flora was deposited 20 Ma.

The most difficult factor to subtract out is ΔMAT_{pg}, or the climate change due to local paleographic changes. This factor does not include the decrease in temperature associated with increased elevation, which is evaluated in equation (5), but includes other effects due to the creation of topography or relief. For example, the creation of topography can contribute to orographic rainfall and latent heating, and can obstruct large-scale air flow. The solar heating over land is often intensified, which modifies values of γ, and magnifies the regional-scale land-sea temperature contrast and thus promotes the development of monsoonal circulation (Meehl, 1992). Sites at the bottom of valleys generally have higher MATs than sites at similar elevation on surfaces of subdued relief (Wolfe, 1992). The ΔMAT_{pg} term is especially difficult to evaluate because one needs information about paleoelevation, the very variable that one is attempting to estimate.

As discussed above, the development of significant Andean elevation probably intensified the quasi-monsoonal circulation. This intensification would most likely cause the Altiplano to become drier. Though more moist air would be drawn from the Amazon as the cordillera grew, these air masses would lose more and more of their moisture on the eastern slope of the Andes before they reached the Altiplano, or be blocked entirely. Today, the highest values of mean annual precipitation in Bolivia are found on the eastern slope, and these rates decrease with elevation, reaching values of 10–50 cm on the Altiplano (Roche, 1992).

Also, increasing uplift would probably further stabilize the subtropical anticyclone over the eastern Pacific ocean and thus intensify the Peru Current, which would also tend to increase aridity (Alpers and Brimhall, 1988). The increased aridity might actually cause the climate of the Altiplano to warm, because presently, mean annual temperatures in this area are strongly influenced by the number of cloudy or rainy days (Johnson, 1976).

Paleogeography also affects values of γ, an important variable in equation (5). Meyer (1986, 1992) calculated local values of γ by compiling temperature data from climate stations in areas of high topographic relief from around the world and observed a mean value of 0.59 ± 0.11°C 100 m^{-1}. Axelrod and Bailey (1976) find values of γ from 0.53–0.58°C 100 m^{-1} with an average of 0.55°C 100 m^{-1} for regions closer to sea level, including Brazil and North Carolina.

Elevation and mean annual temperature data for the central Andes was shown in Fig. 10. The effect of

the Peru Current can be clearly seen; sites from the west coast and the western slope of the Andes have significantly cooler MATs than sites from the same altitude on the east side of the Andes. Linear regression analysis of the MAT data from the Altiplano, Cordillera Oriental, and eastern lowlands indicates that the area has an average γ value of 0.43 ± 0.11°C 100 m^{-1}.

This "terrestrial lapse rate" is lower than those observed by Meyer (1986, 1992) and Axelrod and Bailey (1976) because of the effect of elevated base level. A large elevated land surface is heated more than a column of air at the same elevation (Parrish and Barron, 1986) and thus terrestrial lapse rates are reduced relative to those in a free-air column. Note that a large area needs to be elevated to cause this effect; an isolated mountain peak will be better equilibrated with atmospheric temperature (Meyer, 1986).

The elevated base level effect and the effect of upwelling along the coast are also evident in the western US. Wolfe (1992) found that this area had a mean lapse rate of 0.28 ± 0.11°C 100 m^{-1} when he compared MAT data from the interior to interpolated coastal temperature at the same latitude.

In this study, the 0.43°C 100 m^{-1} value for γ is more appropriate to use in equation (5) than the average global values calculated by Meyer (1992) and Axelrod and Bailey (1976), because presently there is an elevated base level effect, and this effect has probably existed since the Cordillera was more than 500–1000 m in height (Wolfe, 1994). However, if the Jakokkota and Potosí floras were deposited at sea level, then during the initial stages of uplift, the temperature would have decreased more rapidly because of the lack of the base level effect. Thus, if the flora was deposited at sea level, using the 0.43°C 100 m^{-1} lapse rate overestimates the amount of uplift slightly, by about 100–300 m, and the estimated Miocene elevation will be too low.

This slight error is preferable to the alternative. If the 0.59°C 100 m^{-1} lapse rate observed by Meyer (1992) is used in equation (5), the amount of uplift would theoretically be underestimated 300 m for every 1000 m the area was uplifted over 500–1000 m. Because the floras are now at elevations around 4000 m, the use of the 0.43°C 100 m^{-1} lapse rate should derive smaller errors.

Additional sources of error

The formal error of the paleoelevation estimate takes into account the 2.1–2.5°C error calculated for the MAT estimates, the error for the modern MAT value (estimated as 0.5°C), and the observed error for γ of $\pm$0.11°C 100 m^{-1}. Using the quotient variance equation, the formal error is calculated to be 1000 m for calculations using the 0.43°C 100 m^{-1} lapse rate and 600 m for calculations using the 0.59°C 100 m^{-1} lapse rate.

The actual error is probably larger. As discussed above, the formal errors for the MAT estimates could be larger due to taphonomic or evolutionary factors. There are errors associated with the changes in MAT due to global cooling, latitudinal continental drift, and paleogeography terms. The potentially large values of these errors make the resulting estimates of paleoelevation preliminary; the results can be refined with collection of coeval sea level floras from Bolivia. However, the results do give a general idea of whether the floras grew nearer to sea level or to their modern elevations, and thus are useful.

The assumption is made that lapse rate does not change significantly with time. This is probably a reasonable conjecture; a comparison of Miocene paleoelevation estimates using the MAT and enthalpy-based altimeters for floras from the western US suggests that Miocene values of γ were similar to modern values (Wolfe *et al.,* 1997). Nonetheless, there is probably some additional error associated with the use of modern values.

The tectonic studies cited above suggest that there was only minor surface deformation in the Altiplano after 10 Ma. Thus, the 10.66 Ma Jakokkota flora, which grew on the Altiplano, should be representative of the late Miocene surface as a whole, not just an isolated fault block. However, it is possible that some faulting occurred after the deposition of the Potosí flora, which could make the paleoelevation estimate less regionally representative.

Results and discussion of elevation analysis

The variables in equation (5) were assigned values as discussed above; the results of the calculation are given in Table 7, and are plotted on Fig. 9. The small values for the global climate change (ΔMAT_{gc}) and latitudinal continental drift (ΔMAT_{pg}) terms suggest that most of the 10.3–13.1°C mean annual temperature change observed between the Miocene and present was due to uplift.

Using the 0.43°C 100 m^{-1} lapse rate, it is estimated that the Jakokkota and Potosí floras grew at paleoelevations of 590–1610 $\pm$ 1000 m and –420–1320 $\pm$ 1000 m, respectively. The range in paleoelevation quoted for each site reflects the ranges given for ΔMAT_{gc} and ΔMAT_{pg}, while the error term is the formal error discussed above. Recall that we chose the most conservative MAT values from those calculated. Because these values imply the least temperature change from the Miocene to the present, they also imply the most conservative values of post-Miocene uplift, and thus represent maximum paleoelevation values.

The lower figure in each paleoelevation range is small enough to suggest that the floras could have

Table 7. Paleoelevation estimates for the Jakokkota and Potosí floras

Parameter	Jakokkota		Potosí	
PaleoMAT of flora (°C)	18.6–21.0	18.6–21.0	21.5–23.3	21.5–23.3
Modern MAT at same site (·C)	8.3	8.3	8.6	8.6
MAT difference (·C)	10.3–12.7	10.3–12.7	12.9–14.7	12.9–14.7
MAT diff. due to global cooling (·C)*	−1 to 1	−1 to 1	−1 to 6	−1 to 6
MAT diff. due to continental drift (·C)*	+0.7	+0.7	+0.9–1.2	+0.9–1.2
MAT diff. due to paleogeography	?	?	?	?
MAT diff. due to elevation change (·C)	10.0–14.4	10.0–14.4	12.8–21.9	12.8–21.9
Value of g (°C/100 m)	0.43	0.59	0.43	0.59
Elevation change (m)	2330–3350	1700–2440	2980–5090	2170–3710
Modern elevation (m)	3940	3940	4300	4300
Miocene Paleoelevation (m)	**590–1610**	1500–2240	**0–1320**	590–2130
Error (m)	1000	600	1000	600

*Negative values indicate a cooling from the Miocene to the present, positive values indicate a warming.

grown near sea level. Thus, as discussed above, the 600 m estimate for the Jakokkota flora could be 100–300 m too low because of the use of the 0.43°C 100 m^{-1} lapse rate. The lower bound of the Potosí flora, an unlikely 420 m below sea level, could be too low because of the 0.43°C 100 m^{-1} lapse rate bias, or because of the wide range in ΔMAT_{gc} values, necessitated by the uncertainty in the age of the flora.

For comparison, paleoelevations estimates using the 0.59°C 100 m^{-1} value for γ are given in Table 7, with a value of 1500–2240 $\pm$ 600 m and 850–2130 $\pm$ 600 m for Jakokkota and Potosí, respectively. These paleoelevations are higher than those estimated using the 0.43°C 100 m^{-1} value for γ, but recall that these calculations underestimate the amount of uplift, around 300 m for every kilometer of uplift over 500–1000. Thus the 0.43°C 100 m^{-1} estimates are preferred.

The values in the elevation change row in Table 6 represent the estimated uplift since the deposition of each flora. The estimate of 2300–3350 $\pm$ 1000 m of uplift since Jakokkota time, is consistent with, though on the high side, of uplift estimates derived by Kennan *et al.* (1997) from river gradients on paleosurfaces; they estimate 2000–2500 m of uplift for the Cordillera Oriental since 10 Ma. This and other non-botanical estimates of Andean uplift will be discussed in detail in a companion paper (Gregory, in preparation).

These new uplift estimates for Jakokkota and Potosí are higher than the original estimates derived by E. W. Berry using the nearest living relative method. Berry studied the Potosí flora along with the Miocene Corocoro flora from the northern Altiplano (near Jakokkota) and the still undated, but probably Miocene, Pislipampa flora from the Cordillera Oriental. By determining the climate/elevation range of the closest living relatives to the fossil species, he estimated at least 1500 m of uplift since the Potosí flora was deposited (Berry, 1939) compared to 3000 to 4300 $\pm$ 1000 m for this study; about 2000 m of uplift after the Corocoro flora was deposited (Singewald and Berry, 1922) compared to 2300–3350 $\pm$ 1000 m for Jakokkota in this study; and between 2000–2700 m of uplift since the Pislipampa flora was deposited (Berry, 1922b).

Tectonic implications

If the paleobotanically-based paleoelevation estimates are taken at face value, they suggest that the Cordillera Occidental was at a low to intermediate elevation in the early–middle Miocene, and that the Altiplano was at an intermediate elevation at 10.7 Ma. The data imply that the Andean Cordillera is young, undergoing a significant component of uplift since the late Miocene.

As shown in Fig. 9, the elevation estimate for the Potosí flora is consistent with all the proposed tectonic models discussed above. However, the paleoelevation estimated for the Jakokkota flora suggests that the Molnar and Lyon Caen (1988) model, in which the Altiplano reaches its present height at 10 Ma, overpredicts the late Oligocene to middle Miocene uplift rate. The elevation estimates of Okaya *et al.* (1997) and Lamb *et al.* (1997) are consistent with, if on the high side, of the Jakokkota estimate, while estimates of Gubbels *et al.* (1993) are well within the elevation range estimated in this study for the Jakokkota flora. Thus the data supports the two-stage models of uplift, which suggest some sort of lower crustal thickening after surface deformation ceased.

Given the large errors on the botanically–based estimates, it is impossible to determine whether the Cordillera uplifted or remained at the same height during the time between the deposition of the two floras. With the proposed compressional regime, it is unlikely that the elevation decreased.

CONCLUSIONS

In this study, we analyzed a new collection of the Jakokkota flora and a sample from the literature of the Potosí flora in order to determine the paleoclimate and paleoelevation of the Miocene Altiplano and Cordillera Oriental. This work has resulted in the following conclusions:

(1) The age of the Jakokkota flora is 10.66 ± 0.06 Ma based on laser fusion $^{40}Ar/^{39}Ar$ dating of a sanidine-bearing tuff located 3 m above the fossiliferous layer.
(2) Comparison of the foliar physiognomy of each flora with the CLAMP 3B database of modern vegetation (Wolfe, 1995) via canonical correspondence analysis and multiple regression analysis implies a subtropical or paratropical-dry climate. We estimate a mean anual temperature of $18.6–21.0 \pm 2.5°C$ for Jakokkota, and $21.5–21.7 \pm 2.1°C$ for Potosí, with a growing season precipitation of around 50 ± 43 cm for both floras. This estimate for the Potosí flora must be considered preliminary, because it is based on a literature sample.
(3) At this time, the enthalpy-based paleoaltimeter of Forest *et al.* (1998) cannot be used to analyze the paleoelevation of floras in the tropics.
(4) A modified form of the mean-annual temperature (MAT) paleoaltimeter implies a paleoelevation of $590–1610 \pm 1000$ m for the Jakokkota flora and $0–1320 \pm 1000$ m for the Potosí flora (Table 7). Taking the modern elevations of 3940 m and 4300 m for Jakokkota and Potosí, respectively, and subtracting the paleoelevation, we derive uplift amounts of 2300–3400 m since 10.7 Ma, and 3000–4300 m since 20.7–13.8 Ma.
(5) The intermediate paleoelevation estimated for Jakokkota is not consistent with the tectonic model by Molnar and Lyon-Caen (1988), in which the Altiplano reaches its present height by 10 Ma and subsequently builds laterally. Rather, it is consistent with two-stage models of uplift (Allmendinger *et al.,* 1997; Lamb *et al.,* 1997; Okaya *et al.,* 1997), in which the Altiplano continues to uplift after surface shortening ceases at ~10 Ma.

Acknowledgements — KMG and KV were supported by U.S. National Science Foundation grant EAR 93-17078. WCM was supported by the New Mexico Bureau of Mines and Mineral Resources. The development of the New Mexico Geochronology Research Laboratory was aided by U.S. National Science Foundation grant EAR-92064438. Many thanks to Jaime Argollo for assistance with relocating the Jakokkota site and for use of laboratory facilities at the Universidad Mayor de San Andres. Adelide Auza and Nelia Dunbar provided assistance in the field. Reviews by R. J. Burnham, C. E. Forest, A. Graham, and J. A. Wolfe significantly improved the manuscript. This is Lamont-Doherty Earth Observatory contribution number 5837.

REFERENCES

Allmendinger, R.W., Jordan, T.E., Kay, S.M. and Isacks, B.L. (1997) The evolution of the Altiplano–Puna plateau of the central Andes. *Annual Reviews of Earth and Planetary Science* **25**, 139–174.

Alpers, C.N. and Brimhall, G.H. (1988) Middle Miocene climatic change in the Atacama Desert, northern Chile: evidence from supergene mineralization at La Escondida. *Geological Society of America Bulletin* **100**, 1640–1656.

Axelrod, D.I. and Bailey, H.P. (1976) Tertiary vegetation, climate and altitude of the Rio Grande depression, New Mexico–Colorado. *Paleobiology* **2**, 235–254.

Barron, J.A. (1984) Diatom paleoceanography and paleoclimatology of the central and eastern Equatorial Pacific between 18 and 16.2 Ma. In *Initial reports of the Deep Sea Drilling Project*, eds Mayer, L. and Theyer, F. pp. 935–945. U.S. Government Printing Office, Washington, D.C., USA.

Beck, S.L., Zandt, G., Myers, S.C., Wallace, T.C., Silver, P.G. and Drake, L. (1996) Crustal-thickness variations in the central Andes. *Geology* **24**, 407–410.

Benjamin, M.T., Johnson, N.M. and Naeser, C.W. (1987) Recent rapid uplift in the Bolivian Andes: evidence from fission track dating. *Geology* **15**, 680–683.

Berry, E.W. (1919) Fossil plants from Bolivia and their bearing upon the age of uplift of the eastern Andes. In *Proceedings U.S. National Museum*, **54**, 103–164.

Berry, E.W. (1922a) Late Tertiary plants from Jancocata, Bolivia. *The John Hopkins University Studies in Geology* **4**, 205–221.

Berry, E.W. (1992b) Pliocene fossil plants from eastern Bolivia. *The John Hopkins University Studies in Geology* **4**, 145–202.

Berry, E.W. (1939) The fossil flora of Potosí. *The John Hopkins University Studies in Geology* **13**, 1–67.

Britton, N.L. (1892) Note on a collection of Tertiary fossil plants from Potosí, Bolivia. *Transactions of the American Institute of Mining Engineering* **21**, 250–259.

Cerling, T.E. (1991) Carbon dioxide in the atmosphere: evidence from Cenozoic and Mesozoic paleosols. *American Journal of Science* **291**, 377–400.

Chaloner, W.G. and Creber, G.T. (1990) Do fossil plants give a climatic signal? *Journal of the Geological Society, London* **147**, 343–350.

Chase, C.G., Gregory-Wodzicki, K.M., Parrish-Jones, J.T. and DeCelles, P. (1998) Topographic history of the western Cordillera of North America and controls on climate. In *Tectonic Boundary Conditions for Climate Model Simulations*, eds Crowley, T.J. and Burke, K. Oxford University Press, Oxford, U.K. (in press).

Coney, P.J. and Evenchick, E.A. (1994) Consolidation of the American Cordilleras. *Journal of South American Earth Sciences* **7**, 241–262.

Dean, J.M. and Smith, A.P. (1979) Behavioral and morphological adaptations of a tropical plant to high rainfall. *Biotropica* **10**, 152–154.

Dunbar, R.B., Marty, R.C. and Baker, P.A. (1990) Cenozoic marine sedimentation in the Sechura and Pisco basins, Peru. *Palaeogeography, Palaeoclimatology, Palaeoecology* **77**, 235–261.

England, P. and Molnar, P. (1990) Surface uplift, uplift of rocks, and exhumation of rocks. *Geology* **18**, 1173–1177.

Forest, C.E., Molnar, P. and Emanuel, K.A. (1995) Palaeoaltimetry from energy conservation principles. *Nature* **374**, 347–350.

Forest, C.E., Wolfe, J.A., Molnar, P. and Emanuel, K.A. (1998) Palaeoaltimetry incorporating atmospheric physics and botanical estimates of paleoclimate. *Geological Society of America Bulletin,* in press.

Francis, P.W., Baker, M.C.W. and Halls, C. (1981) The Kari Kari Caldera, Bolivia, and the Cerro Rico Stock. *Journal of Volcanology and Geothermal Research* **10**, 113–124.

GEOBOL (1994) Mapa Geologico del Area Berenguela: Hojas Santiago de Machaca-Charana-Thola Kkollu. *Publicacion especial Boletin 4*. GEOBOL, La Paz, Bolivia.

Givnish, T. (1979) On the adaptive significance of leaf form. In *Topics in Plant Population Biology*, eds Solbrig, O.T., Jain, S.,

Johnson, G.B. and Raven, P.H., pp. 375–407. Columbia University Press, New York, USA.

Givnish, T.J. (1984) Leaf and canopy adaption in tropical forests. In *Physiological Ecology of Plants of the Wet Tropics*, eds Medina, E., Mooney, H.A. and Vazquez-Yanes, C., pp. 51–84. Dr. W Junk, The Hague, Netherlands.

Givnish, T.J. (1987) Comparative studies of leaf form: assessing the relative roles of selective pressures and phylogenetic constraints. *New Phytologist* **106**, 131–160.

Grant, J.N., Halls, C., Salinas, W.A. and Snelling, N.J. (1979) K-Ar ages of igneous rocks and mineralization in part of the Bolivian tin belt. *Economic Geology* **74**, 838–851.

Greenwood, D.R. (1992) Taphonomic constraints on foliar physiognomic interpretations of late Cretaceous and Tertiary palaeoclimates. *Reviews of Palynology and Palaeobotany* **71**, 149–190.

Gregory, K.M. (1994) Palaeoclimate and palaeoelevation of the 35 Ma Florissant flora, Front Range, Colorado. *Palaeoclimates* **1**, 23–57.

Gregory, K.M. (1996) Are paleoclimate estimates biased by foliar physiognomic responses to increased atmospheric CO_2? *Palaeogeography, Palaeoclimatology, Palaeoecology* **124**, 39–51.

Gregory, K.M. and Chase, C.G. (1994) Tectonic and climatic significance of a late Eocene low-relief, high-level geomorphic surface, Colorado. *Journal of Geophysical Research* **99**, 20141–20160.

Gregory, K.M. and McIntosh, W.C. (1996) Paleoclimate and Paleoelevation of the Oligocene Pitch-Pinnacle flora, Sawatch Range, Colorado. *Geological Society of America Bulletin* **108**, 545–561.

Gubbels, T.L., Isacks, B.L. and Farrar, E. (1993) High-level surfaces, plateau uplift, and foreland development, Bolivian Central Andes. *Geology* **21**, 695–698.

Guilderson, T.P., Fairbanks, R.G. and Rubenstone, J.L. (1994) Tropical temperature variations since 20,000 years ago: modulating interhemispheric climate change. *Science* **263**, 663–665.

Hickey, L.J. (1973) Classification of the architecture of dicotyledonous leaves. *American Journal of Botany* **60**, 17–33.

Horton, B.K. and DeCelles, P.G. (1997) The modern foreland basin system adjacent to the Central Andes. *Geology* **25**, 895–898.

Hooghiemstra, H. (1989) Quaternary and upper-Pliocene glaciations and forest development in the tropical Andes: evidence from a long high-resolution pollen record from the sedimentary basin of Bogotá, Columbia. *Palaeogeography, Palaeoclimatology, Palaeoecology* **72**, 11–26.

Isacks, B.L. (1988) Uplift of the Central Andean Plateau and bending of the Bolivian Orocline. *Journal of Geophysical Research* **93**, 3211–3231.

Jacobs, B.F. and Deino, A.L. (1996) Test of climate-leaf physiognomy regression models, their application to two Miocene floras from Kenya and $^{40}Ar/^{39}Ar$ dating of the Late Miocene Kapturo site. *Palaeogeography, Palaeoclimatology, Palaeoecology* **123**, 259–271.

Johnson, A.M. (1976) The Climate of Peru, Bolivia, and Ecuador. In *Climates of Central and South America*, ed. W. Schwerdtfeger, 147–202. Elsevier, New York, USA.

Jordan, G.J. (1997) Uncertainty in palaeoclimatic reconstructions based on leaf physiognomy. *Australian Journal of Botany* **45**, 527–547.

Jordan, T.E., Isacks, B.L., Allmendinger, R.W., Brewer, J.A., Ramos, V.A. and Ando, C.J. (1983) Andean tectonics related to geometry of subducted Nazca plate. *Geological Society of America Bulletin* **94**, 341–361.

Kennan, L., Lamb, S.H. and Hoke, L. (1997) High-altitude palaeosurfaces in the Bolivian Andes: evidence for late Cenozoic surface uplift. In *Palaeosurfaces: Recognition, Reconstruction and Palaeoenvironmental Interpretation*, ed. Widdowson, M., pp. 307–323. The Geological Society Special Publication no. 120.

Lamb, S. and Hoke, L. (1997) Origin of the high plateau in the Central Andes, Bolivia, South America. *Tectonics* **16**, 623–649.

Lamb, S., Hoke, L., Kennan, L. and Dewey, J. (1997) Cenozoic evolution of the Central Andes in Bolivia and northern Chile. In *Orogeny Through Time*, eds Burg, J.P. and Ford, M., pp. 237–264. The Geological Society Special Publication no. 121.

Lenters, J.D. and Cook, K.H. (1995) Simulation and diagnosis of the regional summertime precipitation climatology of South America. *Journal of Climate* **8**, 2988–3005.

Lenters, J.D., Cook, K.H. and Ringler, T.D. (1995) Comments on "On the influence of the Andes on the general circulation of the Southern Hemisphere". *Journal of Climate* **8**, 2113–2115.

Loutit, T.S., Kennett, J.P. and Savin, S.M. (1983) Miocene equatorial and southwest Pacific paleoceanography from stable isotope evidence. *Marine Micropalaeontology* **8**, 215–233.

Marshall, L.G., Swisher, C.C., III, Lavenu, A., Hoffstetter, R. and Curtis, G.H. (1992) Geochronology of the mammal-bearing late Cenozoic on the northern Altiplano, Bolivia. *Journal of South American Earth Sciences* **5**, 1–19.

Matthews, R.K. and Poore, R.Z. (1980) Tertiary $\partial^{18}O$ record and glacio-eustatic sea-level fluctuation. *Geology* **8**, 501–504.

Meehl, G.A. (1992) Effect of tropical topography on global climate. *Annual Reviews in the Earth and Planetary Sciences* **20**, 85–112.

Meyer, H.W. (1986) An evaluation of the methods for estimating paleoaltitudes using Tertiary floras from the Rio Grande Rift vicinity, New Mexico and Colorado. Ph.D. University of California at Berkeley, Berkeley, USA.

Meyer, H.W. (1992) Lapse rates and other variables applied to estimating paleoaltitudes from fossil floras. *Palaeogeography, Palaeoclimatology, Palaeoecology* **99**, 71–99.

Molnar, P. and Lyon-Caen, H. (1988) Some simple physical aspects of the support, structure and evolution of mountain belts. In *Processes in Continental Lithospheric Deformation*, eds Clark, S.P.J., Burchfiel, B.C. and Suppe, J., pp. 179–207. Geological Society of America, Boulder, Colorado, USA, Special Paper 218.

Okaya, N., Tawackoli, S. and Giese, P. (1997) Area-balanced model of the late Cenezoic tectonic evolution of the central Andean arc and back arc (lat 20°–22°S). *Geology* **25**, 367–370.

Parrish, J.T. and Barron, E.J. (1986). *Paleoclimates and Economic Geology*. Society of Economic Paleontologists and Mineralogists Short Course 18.

Roche, M-A. (1992) El Clima de Bolivia. In *Seminario PHICAB*, eds Roche, M.A., Bourges, J., Salas, E. and Diaz, C., pp. 81–93. CONAPHI-IHH-ORSTOM-SENAMHI, La Paz, Bolivia.

Ronchail, J. (1985) *Situations meteorologiques et variations climatologiques en Bolivie*. PHICAB-SENAMHI-IFEA-AASANA-ORSTOM, La Paz, Bolivia.

Roth, J.L. and Dilcher, D.L. (1978) Some considerations in leaf size and leaf margin analysis of fossil leaves. *Courier Forschungsinstitut Senckenberg* **30**, 165–171.

Russo, R.M. and Silver, P.G. (1996) Cordillera formation, mantle dynamics, and the Wilson cycle. *Geology* **24**, 511–514.

Samson, S.D. and Alexander, C.E. (1987) Calibration of the interlaboratory 40Ar/39Ar dating standard, Mmhb-1. *Isotope Geoscience* **66**, 27–34.

Savin, S.M. (1977) The history of the earth's surface temperature during the past 100 million years. *Annual Reviews in Earth and Planetary Science* **5**, 319–355.

Savin, S.M., Douglas, R.G. and Stehli, F.G. (1975) Tertiary marine paleotemperatures. *Geological Society of America Bulletin* **86**, 1499–1510.

Savin, S.M., Abel, L., Barrera, E., Hodell, D., Kennett, J.P., Murphy, M., Keller, G., Killingley, J. and Vincent, E. (1985) The evolution of Miocene surface and near-surface marine temperatures: Oxygen isotopic evidence. In *The Miocene Ocean, Paleoceanography and Biogeography,* ed. Kennett, J.P. Geological Society of America, Memoir, 163, 49–82.

Sempere, T., Hérail, G., Oller, J. and Bonhomme, M.G. (1990) Late Oligocene-early Miocene major tectonic crisis and related basins in Bolivia. *Geology* **18**, 946–949.

Sempere, T., Butler, R.F., Richards, D.R., Marshall, L.G., Sharp, W. and Swisher, C.C., III. (1997) Stratigraphy and chronology of upper Cretaceous–lower Paleogene strata in Bolivia and northwest Argentina. *Geological Society of America Bulletin* **109**, 709–727.

Sheffels, B.M. (1990) Lower bound on the amount of crustal shortening in the central Bolivian Andes. *Geology* **18**, 812–815.

Singewald, J.T. and Berry, E.W. (1922) The Geology of the Corocoro Copper District of Bolivia. *The John Hopkins University Studies in Geology* **1**, 1–117.

Sirvas, F. and Torres, E. (1966) Consideraciones geológicas de la zona noroeste de la provincia Pacajes del Departamento de La Paz. *Boletín del Instituto Boliviano del Petroleo* **6**, 54–64.

Smith, A.G., Hurley, A.M. and Briden, J.C. (1981) *Phanerozoic paleocontinental world maps*. Cambridge University Press, Cambridge.

Suarez, Soruco R. and Diaz, Martinez E. (1996) *Lexico estratigrafico de Bolivia*. Revista Technica de Yacimientos Petroliferos Fiscales Bolivianos 17.

Taggart, R.E. and Cross, A.T. (1990) Plant successions and interruptions in Miocene volcanic deposits, Pacific Northwest. In *Volcanism and fossil biogas*, eds Lockley, M.G. and Rice, A., pp. 57–68. Geological Society of America, Boulder, Colorado, USA, Special Paper 244.

Taylor, S.E. (1975) Optimal leaf form. In *Perspectives of Biophysical Ecology*, eds Gates, D.M. and Schmerl, R.B., pp. 73–86. Springer Verlag, New York, U.S.A.

Tosdal, R.M., Clark, A.H. and Farrar, E. (1984) Cenozoic polyphase landscape and tectonic evolution of the Cordillera Occidental, southernmost Peru. *Geological Society of America Bulletin* **95**, 1318–1332.

Van Der, Burgh J., Visscher, H., Dilcher, D.L. and Kürschner, W.M. (1993) Paleoatmospheric signatures in Neogene fossil leaves. *Science* **260**, 1788–1790.

Vandervoort, D.S., Jordan, T.E., Zeitler, P.K. and Alonso, R.N. (1995) Chronology of internal drainage development and uplift, southern Puna plateau, Argentine central Andes. *Geology* **23**, 145–148.

Vose, R.S., Schmoyer, R.L., Steurer, P.M., Peterson, T.C., Heim, R., Karl, T.R. and Eischeid, J.K. (1992) The Global Historical Climatology Network: Long-Term Monthly Temperature, Precipitation, Sea Level Pressure, and Station Pressure Data. In *CDIAC's Numeric Data Package Collection*, version 1.02. Oak Ridge National Laboratory, Oak Ridge, Tennessee, U.S.A.

Walsh, K. (1994) On the influence of the Andes on the general circulation of the Southern Hemisphere. *Journal of Climate* **7**, 1019–1025.

Webb, L.J. (1968) Environmental relationships of the structural types of Australian rain forest vegetation. *Ecology* **49**, 296–311.

Wilf, P. (1997) When are leaves good thermometers? *Paleobiology* **23**, 373–390.

Wing, S.L. and Greenwood, D.R. (1993) Fossils and fossil climate: The case for equable continental interiors in the Eocene. In *Paleoclimates and Their Modelling with Special Reference to the Mesozoic Era*, eds Allen, J.R.L., Hoskins, B.K., Sellwood, B.W. and Spicer, R.A., pp. 243–252. Philosophical Transactions of the Royal Society, London, B. biological sciences, London.

Wolfe, J.A. (1971) Tertiary climatic fluctuations and methods of analysis of Tertiary floras. *Palaeogeography, Palaeoclimatology, Palaeoecology* **9**, 27–57.

Wolfe, J.A. (1979) Temperature parameters of humid to mesic forests of eastern Asia and relation to forests of other regions of the Northern Hemisphere and Australasia. *United States Geological Survey Professional Paper* **1106**, 37 pp.

Wolfe, J.A. (1992) An analysis of present-day terrestrial lapse rates in the western conterminous United States and their significance to paleoaltitudinal estimates. *United States Geological Survey Professional Paper* **1964**, 35 pp.

Wolfe, J.A. (1993) A method of obtaining climatic parameters from leaf assemblages. *United States Geological Survey Professional Paper* **2040**, 71 pp.

Wolfe, J.A. (1994) Tertiary climate changes at middle latitudes of western North America. *Palaeogeography, Palaeoclimatology, Palaeoecology* **108**, 195–205.

Wolfe, J.A. (1995) Paleoclimatic estimates from Tertiary leaf assemblages. *Annual Reviews in Earth and Planetary Science* **23**, 119–142.

Wolfe, J.A., Herman, A.B. and Spicer, R.A. (1996) Inferring climatic parameters for Cretaceous & Tertiary leaf assemblages using CLAMP (Climate-Leaf Analysis Multivariate Program). *International Organisation of Palaeobotany, Fifth Quadrennial Conference, Santa Barbara, CA, Abstracts*, 113.

Wolfe, J.A. and Schorn, H.E. (1990) Taxonomic revision of the spermatopsida of the Oligocene Creede Flora, Southern Colorado. *United States Geological Survey Bulletin* **1923**, 40 pp.

Wolfe, J.A. and Upchurch, G.R. Jr. (1987) North American nonmarine climate and vegetation during the late Cretaceous. *Palaeogeography, Palaeoclimatology, and Palaeoecology* **61**, 33–77.

Wolfe, J.A., Schorn, H.E., Forest, C.E. and Molnar, P. (1997) Palaeobotanical evidence for high altitudes in Nevada during the Miocene. *Science* **276**, 1672–1675.

Zandt, G., Beck, S.L., Ruppert, S.R., Ammon, C.J., Rock, D., Minaya, E., Wallace, T.C. and Silver, P.G. (1996) Anomalous crust of the Bolivian Altiplano, Central Andes: constraints from broadband regional seismic waveforms. *Geophysical Research Letters* **23**, 1159–1162.

Zartman, R.E. and Cunningham, C.G. (1995) U-Th-Pb zircon dating of the 13.8 Ma dacite volcanic dome at Cerro Rico de Potosí, Bolivia. *Earth and Planetary Science Letters* **133**, 227–237.

APPENDIX

Descriptions of angiosperm forms

Terminology is from (Hickey, 1973). Abbreviations for physiognomic states given in Table 3, definitions from Wolfe (1993):

Species 1 (primary specimen 96.22)

Description

Margin untoothed. Length from 0.5 to 1.7 cm, width from 0.5 to 0.9 cm (L1 to m1). L:W 1–2:1. Apex: ARn. Base: BRn. Shape: SEl, SOv.

Venation

Pinnate, brochidodromous. Midrib massive at base, thinning to moderate. Secondaries moderate, curved, forming a series of festooned loops near the margin. Angle of divergence wide at base, becoming narrow apically. Tertiaries strongly percurrent, most commonly simple, straight or curved. Tertiaries perpendicular to secondaries, oblique to the midvein at the base, with the angle decreasing apically. Quaternaries random reticulate, aereoles imperfect, small.

Comments

96.244 may represent a different form, because the secondaries appear to be closer spaced and have less narrow angles of divergence near the apex, but is not well enough preserved to warrant inclusion as a separate form.

Species 2 Polylepis sp. (primary specimens 96.198, 96.272, 96.347, 96.485)

Description

Margin toothed. Teeth large, round, usually only on apical half of laminae. Teeth vary from close to distant, and from regularly spaced to irregularly spaced. Tip of tooth where vein enters occasionally emarginate. Length from 0.4 to 0.7 cm, width from 0.2 to 0.5 cm (nano to L2). L:W 1–3:1. Apex: ARn. Base: varies from BC to BRn to BAc. Shape: varies from SOb to SEl to SOv.

Venation

Pinnate, mostly craspedodromous, but occasionally some secondaries are semi-craspedodromous. Basal secondaries generally craspedodromous. Midrib stout, thinning to moderate. Secondaries either straight or slightly curved, arising at moderate, uneven angles to the midrib, which decrease apically. Some secondaries, generally the basal secondaries, looped, with a branch from the center of the loop, entering the tooth medially. Some secondaries simple, entering tooth medially. Other secondaries branched, with one branch entering tooth medially, the other branch entering the sinus, or less commonly the adjacent tooth. Often the branch which enters the sinus continues to form a loop that borders the tooth. Simple secondaries have curved branches which enter both adjacent sinuses or join adjacent branches, forming a loop at the tip of the tooth. Some intersecondaries present. Tertiaries moderate, generally strongly percurrent, oblique to the midrib with the angle often decreasing marginally, and straight or more commonly curved. Quaternaries random reticulate, with imperfect aereolation.

Comments

This, along with species 6, the first legume form, is one of the two most common leaves at Jakokkota. The texture of the fossils suggests that the leaf was probably coriaceous. This form has larger and more prominent teeth than *Polylepis tomentellafolia* of Berry (1922a), and appears more likely to correspond with the other Rosaceous form described by Berry (1922a), *Osteomeles kozlowskiana*.

Species 3 (primary specimen 96.7)

Description

Margin untoothed. Length at least 1.4 cm, width 0.6 cm (L2-m1). L:W ratio: 2–3:1. Apex: missing. Base: BAc. Shape: SEl.

Venation

Pinnate, festooned brochidodromous. Midrib massive at base thinning to moderate. Basal secondaries fairly straight, becoming curved apically. Secondaries form loops which join the superadjacent secondary at an acute angle, then forming festooned loops at the margin. Angle of divergence from the midrib almost a right angle at the base, decreasing slightly apically. Tertiaries moderate, straight or curved, strongly percurrent, opposite, mostly RR of Hickey. Oblique to midrib. Quaternary veins random reticulate. Finer venation obscure.

Comments

This species is only based on one fragment, but this fragment is well preserved and thus warrants assignment to a separate species. The festooned brochidodromous margin and very wide angles of divergence of the secondaries makes this species distinct from 12. The texture of the fossil suggests that the leaf was coriaceous.

Species 4 (primary specimens 96.27, 96.159)

Description

Margin untoothed. Length from 2.0 to 4.1 cm, width from 0.5 to 0.9 cm (m1). L:W ratio: 2–>4:1. Apex: AAc. Base: BAc. Shape: SEl.

Venation

Pinnate, brochidodromous. Midrib moderate. Secondaries irregular in course and spacing, with straight, curved or sinuous courses. Angles of divergence variable, but generally narrow. Secondaries fuse into intramarginal vein. Composite intersecondaries fairly common. Tertiaries random reticulate. Quaternary veins also appear to be random reticulate.

Comments

The texture of the fossils suggests that this species has thin, papery leaves.

Species 5–legume 1 (primary specimen 96.441)

Description

Margin untoothed. Length of leaflets from 0.9 to 1.6 cm, width from 0.3 to 0.6 cm (L2-m1). L:W ratio: 2–4:1. Apex: ARn. Base: asymmetrical, with one side BRn and the other BAc. Shape: SEl or SOv. Leaflets asymmetrical.

Venation

Pinnate, brochidodromous. Midrib weak. Secondaries thick, curved or less commonly recurved, forming loops. Spacing irregular. Secondaries join the superadjacent secondary at essentially a right angle. Angle of divergence acute. Higher order venation obscure. Pulvinus has striations.

Comments

These leaves are legumes, as demonstrated by the striations on the pulvinus. They are distinguished from the other two legume species, which both have one prominent secondary loop, by the more subequal secondary loops. It was not possible to identify this species to genus, because legume identification is more based on spines and fruits, while foliage can be extremely similar between species. The asymmetric shape of the lamina suggests that the fossils represent leaflets.

Species 6–legume 2 (primary specimens 96.329, 96.489)

Description

Margin untoothed. Length of leaflet from 0.3 to at least 0.9 cm, width from 0.05 to 0.3 cm (nano-L2). L:W ratio: 2–>4:1. Apex: ARn. Base: Either BRn, or asymmetrical with one side BRn and the other BAc. Shape: SOb or SEl. Some leaflets asymmetrical.

Venation

Pinnate, brochidodromous. Midrib moderate. Basal secondary form very elongate loop, with smaller loops above. Angle of divergence narrow at base, wide to almost a right angle near the apex. Tertiaries random reticulate.

Comments

The striated pulvinus suggests that this species is a legume. It is distinguished from the other two species by the strong primary secondary loop, and the lack of third order loops. The asymmetry of the fossils suggests that they represent leaflets, and their texture suggests that they were hairy and coriaceous. This form probably corresponds to *Calliandra jancocatana* of Berry (1922a).

Species 8: (primary specimen 96.30)

Description

Margin toothed. Teeth acute (B1 or C1 of Hickey), and distantly spaced. Spacing varies between regular and irregular. Length from at least 1.2 to at least 4.5 cm, width from 0.4 to 0.9 cm (L2-m2). L:W ratio: 3–>4:1. Apex: ARn or AAc. Base: BAc. Shape: SOb or SEl.

Venation

Pinnate, semicraspedodromous. Midrib stout at base. Secondaries moderate, curved, fairly widely spaced, running tangent to the margin for a significant distance as a series of loops. Angles of divergence narrow. Branches from these loops enter the teeth medially. Tertiaries fairly straight, strongly percurrent, almost at right angles to the midrib. Higher order venation obscure.

Species 9 (primary specimen 96.31)

Description

Margin toothed. Teeth large, distant and regularly spaced, probably triangular in shape (B2 of Hickey). Length at least 2.4 cm, width at least 1.4 cm (m1-m2). L:W ratio: 1–3:1. Apex: missing. Base: BAc. Shape: SEl.

Venation

Pinnate, probably craspedodromous. Midrib stout. Secondaries mostly obscure. They appear to diverge at wide angles near the base, decreasing rapidly to very acute angles.

Comments

Neither of the specimens are very well preserved, but the distinctive large, widely spaced teeth warrant their inclusion as a separate species. The fossil leaves appear to have had a coriaceous texture.

Species 10: (primary specimen 96.70)

Description

Margin untoothed. Length from 0.3 to at least 1.3 cm, width from 0.2 to 0.6 cm (nano-m1). L:W ratio: 1–4:1. Apex: ARn or AAc. Base: BRn or BAc. Shape: SEl or SOv.

Venation

Pinnate, brochidodromous. Midrib strong. 7–8 pairs of secondaries, diverging from the midrib at wide angles at the base, decreasing to narrow angles near the apex. Secondaries moderate, closely spaced, curved, near the margin becoming a train of loops tangent to the margin. Tertiaries straight, strongly

percurrent, closely spaced, oblique to midrib. Finer venation obscure.

Species 11: (primary specimens 96.204, 96.205)

Description

Margin untoothed. Length from 0.6 to at least 2.5 cm, width from 0.3 to 0.6 cm (L1-m1). L:W ratio: 2–>4:1. Apex: ARn or AAc. Base: BRn or BAc. Shape: SEl or SOv.

Venation

Pinnate, brochidodromous. Midrib stout. Secondaries can be straight, curved, or slightly recurved. The divergence angle is generally wide, though some leaves are asymmetric across the midrib, and one side can have secondaries with a moderate angle of divergence. The secondaries appear to form loops which have merged into an intramarginal vein, making some secondaries appear to be branched. Higher order venation obscure.

Comments

This species is distinguished from species 33 in having stouter secondaries which are curved and often branch and diverge at wider angles. The secondaries are less regular in spacing and divergence angle. This species was probably rather thin, because most of the specimens are torn. Also, the asymmetry of many of the specimens suggests that they are leaflets.

Species 12: (primary specimen 96.72)

Description

Margin untoothed. Length from 1.1 to 2.0 cm, width from 0.3 to 0.8 cm (L2-m1). L:W ratio: 2–4:1. Apex: ARn or AAc. Base: BRn or BAc. Shape: SEl or SOv.

Venation

Pinnate, brochidodromous. Midrib moderate. Secondaries diverge at moderate to narrow angles at the base, becoming more narrow apically. Secondaries stout, curved, joining the superadjacent secondary at an obtuse angle, so that the secondary loops appear to join to form a vein paralleling the margin. Basal secondaries do not join with an obtuse angle, but rather form a loop train which parallels the margin. Tertiaries straight or curved, strongly percurrent, generally oblique to the midrib, with angle remaining fairly constant. Higher order venation obscure.

Comments

This species is distinct from species 3, most obviously because the secondaries join the superadjacent secondaries with an obtuse angle, while in species 3, the secondaries join in a series of loops.

Species 13: (primary specimen 96.236)

Description

Margin untoothed. Length from 0.9 to 3.2 cm, width from 0.4 to 0.9 cm (L2-m1). L:W ratio: 1–>4:1. Apex: ARn or AAc. Base: BRn or BAc. Shape: SOb or SEl.

Venation

Pinnate, brochidodromous. Midrib moderate. Secondaries strong, recurved to variable degrees of less commonly straight, with moderate to narrow angles of divergence. Spacing and angle of divergence varies irregularly. Secondaries closely spaced. Most secondaries branched, with both branches fused into an intramarginal vein. Higher order venation obscure, tertiaries perhaps perpendicular to midrib.

Species 14: Berberis (primary specimen 96.215)

Description

Margin untoothed. Length from 0.5 to 1.7 cm, width from 0.25 to 0.6 cm (L1-m1). L:W ratio: 1–>4:1. Apex: ARn to AAc. Base: truncate (BAc). Shape: SOb to SEl.

Venation

Pinnate, basal, imperfect acrodromous. Midrib moderate. Pseudoprimaries arise at extremely narrow angle to midrib, and continue for at least 1/2 the laminae, forming a large elongate loop close to the midrib. Secondaries arise at wide angles of divergence, with alternating reaches of curved and straight courses. Third order loops surround the secondaries. Tertiaries form a random reticulate net. Higher order venation obscure.

Comments

The pseudoprimaries and spinose teeth suggest the assignment to *Berberis*.

Species 17: (primary specimen 96.142)

Description

Margin untoothed, slightly revolute. Length from 0.4 to 0.9 cm, width from 0.2 to 0.3 cm (nano-L1). L:W ratio: 2–4:1. Apex: ARn to AAc. Base: BRn to BAc. Shape: SEl to SOv.

Venation

Pinnate, brochidodromous. Midrib massive. Secondaries curved, closely spaced, forming loops.

Angle of divergence moderate. Higher order venation obscure.

Comments

This small leaf is distinguishable from species 6 (Legume 2) because of the thick midrib, the wider angle of divergence of the secondaries, and the long (up to 2 mm) petiole which lacks striations. The texture of the fossils suggests that the leaves were coriaceous.

Species 18: (primary specimen 96.143)

Description

Margin untoothed. Length from 0.4 to 0.5 cm, width from 0.3 to 0.4 cm (nano-L2). L:W ratio: 1–3:1. Apex: ARn. Base: BRn, BAc. Shape: SEl.

Venation

Pinnate, brochidodromous. Midrib stout. 3–4 pairs of secondaries, thick, curved, with moderate angles of divergence, remaining fairly constant from base to apex, forming large brochidodromous loops. Higher order venation obscure.

Comments

This form is similar to form 10, but is distinguished as a separate form because of the fewer and wider spaced pairs of secondaries.

Species 19: Berberis (primary specimens 96.171, 96.238)

Description

Margin toothed, with one large, spinose, triangular tooth (type C3) on each side. The two teeth and the apex of the leaf are darkened in specimen 96.171, suggesting that the teeth were hardened, like a bristle. Length 1.5 cm and greater, width from 0.4 to 1.0 cm (L2 to m1). L:W ratio: 1–3:1. Apex: AAc. Base: cuneate. Shape: SOb to SEl.

Venation

Pinnate, semicraspedodromous. Midrib stout, thins markedly at junction with second pair of secondaries. Secondaries curved, angle of divergence narrow. First pair of secondaries parallels margin and forms a train of loops. Second pair of secondaries forms a prominent, elongate loop in the center of the leaf. A branch from this loop enters the tooth medially. Tertiaries appear to form random reticulate net.

Comments

Note that spinose forms are scored in the "no teeth" character state (Wolfe 1993). This form is distinguishable from form 14 because it lacks the basal pseudoprimaries.

Species 22: (primary specimen 96.260, 96.440)

Description

Margin toothed. Teeth very small, round to appressed, regularly and distantly spaced, with gland at tip. Length from 1.0 to at least 2.2 cm, width from 0.2 to 1.0 cm (L1-m1). L:W ratio: 2–>4:1. Apex: ARn, AAc. Base: BAct. Shape: SOb, SEl.

Venation

Pinnate, semicraspedodromous. Midrib moderate. Venation typically obscure; secondaries appear to be curved, arising at narrow angles to the midrib.

Comments

The venation is difficult to see in this form, but the distinctive small, regularly spaced teeth with glands at the tip warrant distinction as a separate form.

Species 25: (primary specimen 96.339)

Description

Margin untoothed. Length from 3 to at least 4.5 cm, width from 1.2 to at least 1.6 cm (m1-m2). L:W ratio: 2–3:1. Apex: AEm, ARn. Base: BAct. Shape: SEl.

Venation

Pinnate, brochidodromous. Midrib moderate. Secondaries moderate, curved, running tangent to the margin for a significant portion of their length, arising at moderate angles of divergence to the midrib. Intersecondaries common. Tertiary veins random reticulate, except for between the basalmost pairs of secondaries, in which they are strongly percurrent and oblique to the midrib. Quaternary veins form random reticulate net.

Comments

This form is made of large brochidodromous leaves. Because of the large size, the specimens are often fragmental, and thus it is difficult to describe the venation. It is possible that these fragments represent more than one species, but not enough detail is present to distinguish them. These fragments are distinct from form 47 because of the more numerous secondaries with wider angles of divergence and the common intersecondaries.

Species 26-Legume 3: (primary specimens 96.279, 96.451)

Description

Margin untoothed. Length from 0.5 to 0.8 cm, width from 0.2 to 0.4 cm (L1-L2). L:W ratio: 1–3:1. Apex: ARn. Base: Asymmetrical, with 1/2 round and

1/2 acute. Shape: SOb. Leaflet is markedly asymmetrical. Pulvinus has striations.

Venation

Pinnate, brochidodromous. Midrib weak. The basal secondaries arise from the base and form large, elongate loops which cover almost the entire laminae; there are two or three such loops on the wide side of the laminae, one loop on the narrow side. These loops are surrounded by third order loops. Secondaries thick compared to the midrib. Higher order venation obscure.

Comments

This form is a legume as evidenced by the striations on the pulvinus. It is distinguished from the other two legume species by the three secondary loops which originate at the base of the laminae. The fossils probably represent leaflets.

Species 28: (primary specimen 96.286)

Description

Margin toothed. Teeth rounded, of variable size, irregularly and distantly shaped. Length 2.5 cm, width from 0.4 to 0.5 cm (m1). L:W ratio: >4:1. Apex: AAct. Base: BAct. Shape: SEl.

Venation

Pinnate, craspedodromous. Midrib stout. Secondaries moderate, curved, straight, or recurved, arising at moderate angles of divergence which remains fairly constant throughout the laminae. Typically, one secondary enters the sinus, while the subjacent secondary joins the margin below the tooth, giving the appearance of a loop with the superadjacent secondary. An intersecondary vein enters the tooth medially. Higher order venation obscure.

Species 30: (primary specimen 96.84)

Description

Margin toothed. Teeth large, rounded, irregularly and distantly spaced. Length from 0.3 to at least 0.4 cm, width at least 0.2 cm (nano-L1). L:W ratio: 2–3:1. Apex: ARn. Base: BRn or BAc. Shape: SEl.

Venation

Pinnate, craspedodromous. Midrib weak. Secondaries thick compared to midrib, curved, arising at moderate to narrow angles of divergence, with the more narrow angles near the apex. Secondaries appear to enter the teeth medially. Tertiary venation difficult to see, but appears to form loops.

Comments

This form is represented only by a few fragments, but the teeth are distinctive enough to warrant a separate form.

Species 33: (primary specimen 96.334)

Description

Margin untoothed. Length up to 2.4 cm, width from 0.4 to 0.5 cm (m1). L:W ratio: >4:1. Apex: AAc. Base: BAc. Shape: SEl. 0.4 cm long petiole.

Venation

Pinnate, brochidodromous. Midrib stout. Secondaries moderate, straight, arising at narrow angles of divergence from the midrib. Secondaries are fused into intramarginal vein. Tertiaries straight, strongly percurrent, oblique to the midrib. Finer order venation obscure.

Comments

This form is distinguished from form 4 by the regularity of the secondaries. It is distinguished from form 11 by the narrow angle of divergence of the secondaries and the well developed intramarginal vein.

Species 40: (primary specimen 96.461)

Description

Margin toothed, sometimes with one small lobe on one side. Teeth large, triangular with an acuminate tip (type D4), closely and regularly spaced, acute. Length from 0.5 to at least 1.8 cm, width from 0.4 to at least 1.2 cm (L1-m2). L:W ratio: 1–2:1. Apex: AAc. Base: BAct. Shape: SOv.

Venation

Pinnate, craspedodromous. Midrib moderate. One side has a strong pseudoprimary which arises at the base and enters lobe. Secondaries are straight to slightly curved, arising at narrow angles of divergence. Secondaries off pseudoprimary slightly recurved. Higher order venation obscure.

Comments

These fossils are often fragmental or curved, thus the details of the venation are difficult to see, but the large, triangular teeth and pseudoprimary make the form very distinctive.

Species 41: (primary specimen 96.474)

Description

Margin untoothed. Length from 0.3 to 0.7 cm, width from 0.1 to 0.3 cm (nano-L2). L:W ratio: 2–4:1. Apex: ARn. Base: BAct. Shape: SOb.

Venation

Pinnate, brochidodromous or mixed craspedodromous. Midrib stout. Secondaries thick, textured, forming a prominent ribbed texture on the leaf. 4–5 pairs, straight, diverging at a very narrow angle to the midrib and either forming an elongate loop which closes near the apex of the leaf or entering tooth medially. Higher order venation obscure.

Species 43: (primary specimen 96.98)

Description

Margin untoothed. Length around 2.2 cm, width from 0.3 to 0.6 cm (L2-m1). L:W ratio: 3– > 4:1. Apex: AAc. Base: BAc. Shape: SEl or SOv.

Venation

Pinnate, brochidodromous. Midrib massive. About 1/5 of the way up the laminae, two pseudoprimaries split from the midrib, one on either side, at an extremely narrow angle of divergence ($< 5^{\circ}$), diminishing the thickness of the midrib by their thickness. These pseudoprimaries are moderate, slightly curved, and apparently run the entire length of the laminae. Two pairs of secondaries diverge at narrow angles below the pseudoprimaries and 5–6 pairs diverge above. The secondaries are moderate in thickness and curved, running tangent to the margin for most of their length. They become lighter and less prominent near the border, forming loops just within the margin. Tertiaries are thin, strongly percurrent, and almost perpendicular to the midrib. The quaternary veins appear to form a random reticulate net.

Comments

The papery thin texture and midrib, which appears to be formed of strands which then split off to become secondaries, are very similar to those of form 4. However, the prominent pseudoprimaries which split off just above the base and run for the entire lamina and the lack of a well defined intramarginal vein distinguish these leaves as a separate form.

Species 45: (primary specimen 96.226)

Description

Margin toothed on apical portion of leaf. Teeth large, regularly and distantly spaced, acute (type C1). Length from around 1 cm, width from 0.3 to 0.4 cm (L2). L:W ratio: 2–3:1. Apex: AAc. Base: missing. Shape: SEl.

Venation

Pinnate, semicraspedodromous or mixed craspedodromous. Midrib moderate. Secondaries not well preserved, but appear to be widely spaced, curved, arising at moderate angles or divergence, forming loops somewhat within the margin. Tertiaries form prominent orthogonal reticulate net. Resulting aereoles are small.

Comments

Even though the primary specimen is fragmental and the secondaries are not well preserved, this is distinguished as a separate form by the large, acute teeth on the apical portion of the leaf, and the prominent but small aereolation formed by the tertiaries.

Species 46: (primary specimen 96.261)

Description

Margin toothed. Teeth broadly rounded (type A1), regularly and closely spaced, with glands in the sinus. Length from at least 1.2 cm, width 0.8 cm (m1). L:W ratio: 1–2:1. Apex: missing. Base: missing. Shape: SEl.

Venation

Pinnate, semicraspedodromous. Midrib moderate, curved. Secondaries moderate, curved, arising at wide angles of divergence and joining the superadjacent secondary in a series of loops. Tertiaries percurrent, sinuous, close, predominantly alternate, almost perpendicular to midrib. Two tertiary branches from the secondary loops enter the sinuses, and several branches enter the teeth. Quaternary veins from orthogonal reticulate net.

Species 47: (primary specimen 96.237)

Description

Margin untoothed. Length from 0.8 to at least 3 cm, width from 0.3 to 1 cm (L2-m2). L:W ratio: 2–4:1. Apex: ARn or AAc. Base: BAc. Shape: SOb or SEl.

Venation

Pinnate, brochidodromous. Midrib stout. 5–6 pairs of secondaries, moderate, curved, widely spaced, with a slightly sinuous course, running tangent to the margin for a significant potion of their course. Secondaries arise at narrow angles of divergence and join the superadjacent secondary in a series of loops. Tertiaries strongly percurrent, oblique to the midrib in the base of the laminae to almost perpendicular to the midrib more apically. Quaternary veins form a random reticulate net.

Species 48: (primary specimen 96.487)

Description

Margin not preserved. Length at least 1 cm, width at least 0.8 cm (m1). L:W ratio: missing. Apex: missing. Base: BRn. Shape: missing.

Venation

Pinnate, probably craspedodromous. Midrib massive. Secondaries thick, straight, arising at wide and fairly constant angles of divergence. Tertiaries thick, straight, strongly percurrent, closely spaced, and oblique to the midrib. Higher order venation obscure.

Comments

The prominent, strongly percurrent, closely spaced, straight tertiaries suggest that this form corresponds to *Alnus preacuminata* of Berry (1922a), but it is unlikely that this form truly is *Alnus*.

Species 49: (primary specimen 96.488)

Description

Margin untoothed. Length at least 1.2 cm, width 0.4 cm (L2-m1). L:W ratio: 3–>4:1. Apex: missing. Base: acute. Shape: SEl.

Venation

Pinnate, brochidodromous. Midrib stout. Secondaries moderate, straight to somewhat curved, closely spaced, arising at narrow angles to the midrib and joining the superadjacent secondary in a series of loops which run tangent to the margin for a significant length of the laminae. Tertiary veins percurrent, curved, predominantly alternate, often forming a composite intersecondary. Quaternary veins form orthogonal reticulate net.

Comments

This form is distinguished from form 10 by the straighter, closer spaced, longer secondaries and the composite intersecondaries.

Species 50: (primary specimen 96.455)

Description

Margin untoothed. Length at least 1 cm, width at least 0.5 cm (L2). L:W ratio: 2–3:1. Apex: missing. Base: missing. Shape: SEl.

Venation

Pinnate, brochidodromous. Midrib stout, sinuous. Secondaries moderate, sinuous or less regularly, curved or straight, forming loops just within the margin, joining the superadjacent secondary in a slightly acute angle. Angle of divergence varies irregularly from 80 to 100°. Spacing irregular. Rare intersecondaries. Tertiaries percurrent, curved or straight, predominantly alternate. Oblique to midvein, with angle decreasing exmedially. Quaternary veins form orthogonal net.

Comments

The distinctive irregularity of the secondaries of this fragment distinguishes the leaf from form 3 and form 48.